The Thermal Interaction between the Atmosphere and the Earth and Propagation of Diurnal Temperature Waves

H. L. KUO

The University of Chicago

(Manuscript received 7 December 1967, in revised form 13 March 1968)

ABSTRACT

The thermal interaction between the atmosphere and the underlying earth, as related to the diurnal heat wave, is investigated through the use of a modified virtual conduction model in which the influences of turbulence and thermal convection are simulated by diffusion while the influence of terrestrial radiation is approximated partly by diffusion and partly by a Newtonian cooling, the ratio between the two parts increasing from summer to winter. The virtual thermal diffusivity is assumed to vary both in time and in space in order to represent the various physical processes involved in accomplishing the actual heat transfer. It is shown that a mean upward transport of heat is maintained through the diurnal variation of the transfer process although the mean lapse rate is stable, thereby removing a long-standing difficulty in evalutating the turbulent heat flux from the mean potential temperature distribution.

The solar energy received at the surface is found to be partitioned into the two media and to space in proportion to the effective heat capacities and the surface radiation factor; the former are defined as 1) the product of the respective heat capacity ρc_p and the square roots of the frequency q and the thermal diffusivity K in case K is constant, and 2) the product of ρc_p and the vertical gradient of K when dK/dz is very large near the surface. Further, a large dK/dz tends to increase the attenuation rate and to reduce the time lag of the temperature wave, therefore tending to maintain a steep temperature gradient at the boundary. The effect of the terrestrial radiation at the surface is to increase the cooling rate in the afternoon and to reduce it during the night, thereby helping to shift the time of the temperature maximum forward.

The analysis also shows that the temperature wave in the lowest few hundred meters of the atmosphere is influenced appreciably by the absorption of the solar radiation and by the interactions between K and T waves, and this is especially so for the mean temperature. Comparison of the theoretical results with observations made at O'Neill in summer shows that the observed temperature wave in the first 500 m can be approximated closely by the solution corresponding to a K profile which increases from a small value (from 3–10 $cm^2\ sec^{-1}$) at the surface to about $10^5\ cm^2\ sec^{-1}$ at 10 m, and by consideration of the direct absorption of solar radiation and K-T interaction terms. The winter observations are approximated very closely by the solutions of the simple one-layer power law diffusivity models without consideration of the absorption of solar radiation and the interaction terms, provided a much larger surface value of the diffusivity is used. These results indicate that the transfer of terrestrial radiation is of importance at the surface in winter.

1. Introduction

Because of the low absorptive power of the earth's atmosphere for short wave solar radiation, only a small fraction of the effective incoming solar energy is absorbed by the atmosphere, the bulk of it being absorbed by the earth's surface. This energy is then transmitted partly downward into the ground and partly upward into the atmosphere, thereby setting up temperature waves in the two media through the quasi-periodic variations of the solar energy at earth's surface. The most conspicuous of these is the diurnal variation. The intent of this paper is to analyze the various factors that determine the nature of the temperature waves in the two adjacent media, such as the partition of heat at the surface, the variation of the surface temperature as a function of the effective solar radiation and other physical parameters, the variations of the amplitudes and phases with the distances from the boundary, and especially, the question of the possibility of predicting these various elements of the temperature waves with a simple mathematical model. This model is based on the K theory of turbulent diffusion and an approximation to the selective absorption of long wave radiation.

In order to better understand the nature of the diurnal temperature waves set up by the solar radiation in the two media, we have presented in Section 2 a set of temperature curves and profiles pertaining to these temperature waves, obtained from measurements made by the Great Plains turbulence project at O'Neill, Nebr., during the summer of 1953. From these observations it is readily seen that the propagation of the temperature wave in the ground may be considered as governed essentially by the classical heat-conduction equation with a nearly constant thermal conductivity, with relatively minor complications due to the variations of these properties with space, time and temperature. On the other hand, even though the propagation of the temperature wave in the atmosphere is commonly treated as a diffusion process, it is actually a rather complex process as

it is accomplished through the joint actions of radiation, ordinary (mechanical) turbulence, and organized and unorganized thermal convections. Each of these processes requires careful and detailed investigation before we can fully understand their total effect.

Even though radiative transfer is mathematically simpler than convection (because it does not involve fluid motion), its direct inclusion together with turbulent diffusion leads to an integral or differential equation of higher order, which is hard to solve when the eddy diffusivity varies with height. We have therefore restricted ourselves in this paper to the treatment of the simplified version of this equation, which is obtained in Section 3 by dividing the absorption spectrum of terrestrial radiation into strongly and weakly absorbed regions, classified in accordance with the local scale of variation or local rate of heating. It is then found that the influence of the strongly absorbed part can be approximated by a diffusion process while that of the weakly absorbed part may be treated as a Newtonian cooling. Further, when a sharp and intense thermal boundary layer is present on account of continued solar radiation (such as during a hot summer day), most of the absorption spectrum will fall into the category of weak absorption, and the radiative diffusivity will therefore be small; whereas, when a sharp thermal boundary layer is not present (such as in winter), part of the spectrum will fall into the strongly absorbed category. Thus, this treatment of the radiative transfer of longwave radiation results in a small value of the radiative diffusivity near the surface during the summer and a large surface radiative diffusivity, on the order of 10^3 cm^2 sec^{-1} during the winter.

Of the three processes mentioned above, thermal convection is of particular importance during a clear summer day, and the question arises as to whether it can be treated as part of turbulence and represented by the K theory; that is, by the product of a thermal diffusivity and the local gradient of the potential temperature. The difficulty of this formal representation becomes evident when one considers the convection currents produced by rapid surface heating. The buoyant elements originating from the hot surface can easily penetrate into the stable layers above and carry heat upward. If the customary diffusion equation is applied directly to the total temperature field, one will then find it necessary to introduce infinite and negative diffusivities at and above the level of inversion of potential temperature in order to give upward heat transport (which does not seem to be meaningful because it can not be applied elsewhere). This difficulty is avoided in the present work by expanding the potential temperature and the eddy conductivity into Fourier series in time, and viewing the process as in gradual progression. This is also developed in Section 3. In this way we find that the various harmonics of the temperature wave are represented adequately by a modified diffusion equation with a time-independent turbulent diffusivity.

Solar radiation and terms representing the interactions between θ and K appear as nonhomogeneous terms in this equation and in the boundary condition. Furthermore, the mean temperature is governed by a second-order differential equation in z with the mean solar radiation and the correlation between the departures of the temperature and the virtual diffusivity as nonhomogeneous heating functions. Since K is large during the day on account of the convective activity, this correlation gives rise to a mean upward transport of heat, whose magnitude is larger than that given by the mean gradient. Hence, the inclusion of this "eddy transport" removes the one long-standing difficulty in determining the mean vertical turbulent heat transfer by using the mean potential temperature gradient (which yields downward instead of upward transport).

In order to gain a better understanding of the processes involved, we first obtain the solutions in Section 4 for the two media by using two different, but constant, thermal diffusivities, and by including a Newtonian cooling and absorption of solar radiation. The Newtonian cooling resulting from longwave radiation is shown to be of little importance for the diurnal heat wave in the atmosphere and so may therefore be neglected, but its influence must be included in the mean temperature equation. In addition, it also reveals that the factors that determine the sharing of the solar energy are the effective heat capacities of the two media and the radiational cooling factor of the ground. The absorption of solar radiation in the atmosphere has also been taken into consideration in this analysis.

In Section 5 we first examine by the use of an approximate solution, the influence of the increase of the thermal diffusivity with height near the surface. It is shown that a large vertical gradient of K increases the attenuation rate and reduces the phase lag of the temperature wave, thereby producing a strong surface thermal boundary layer. In this case the effective heat capacity of the atmosphere and the attenuation rate are determined by the gradient of K, and not by K itself.

These conclusions are confirmed by the exact solutions obtained in the latter part of Section 5, where the variation of K with height in the atmosphere is represented by a multi-layer mode. The influences of K values at upper levels are also felt in the lowest layer.

In Section 6 the effect of the variation of K with time resulting from the convective activity is analyzed by the perturbation method. To the first order, the influence of the diurnal variation of the diffusivity K is represented by the product of the mean temperature gradient and the variable part of K, and one important consequence of this influence is a shift of the time of the temperature maximum and minimum forward at higher levels.

The determination of the variation of the mean temperature θ_0 with height is discussed in Section 7. In the first few hundred meters θ_0 is determined essentially by the balance between the absorption of solar radiation,

the Newtonian cooling, and by the correlation between the diffusivity and the temperature field. The influence of the first two factors is to produce a stable, nearly isothermal stratification, while the combined influence of the last two is to create a boundary-layer type, unstable stratification. The net effect of these three processes is to maintain a stable mean lapse rate above a thin boundary layer within which the mean lapse rate may be nearly adiabatic.

The test of the theory against the observations at O'Neill is given in the first part of Section 8. Assuming that K increases rapidly from a small value at the surface to about 10^5 cm^2 sec^{-1} at the 10-m level and then to its maximum of about 5×10^5 cm^2 sec^{-1} at $z=200$ m, we show that the observed temperature waves within the first 20 m in the atmosphere and in the ground at O'Neill are closely represented by the solution, both in amplitude and in phase. At greater altitudes it is necessary to take into consideration the absorption of direct solar radiation and the first-order interaction between the diurnal variations of the temperature and of the diffusivity in order to achieve a better agreement between the theory and the observations, especially in regard to the phase variation. From the smallness of the surface values of K (from 3–6 cm^2 sec^{-1}) needed to bring agreement between theory and observations, we conclude that radiative diffusivity is absent for these cases. Similar conclusions are reached from other summer observations.

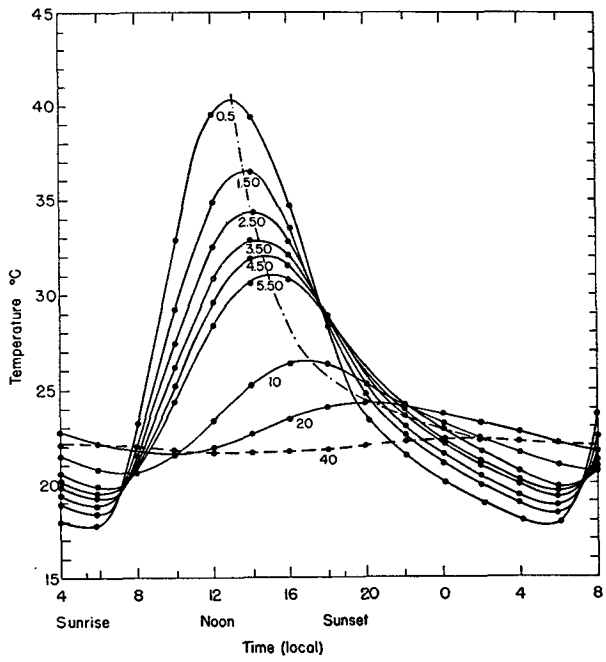

FIG. 1a. Average diurnal temperature variations at various depths (in cm) in the ground, based on The University of Texas observations from 0.5–5.5 cm and The Johns Hopkins University observations below 10 cm taken at O'Neill, Nebr., summer 1953. The dash-dot curve represents the locus of the temperature maxima.

Similarly, comparison between theory and observations under winter conditions are made in the latter part of Section 8. Here it is found that the temperature waves during the winter are closely approximated by the solutions for a rather simple K profile; namely, a single-layer, $p=4/3$ profile with a much larger K value at the surface, of the order of 2×10^3 cm^2 sec^{-1}, while at greater heights $K<10^5$ cm^2 sec^{-1}. These results indicate that the influence of the longwave radiation by the strongly absorbed part of the spectrum is prominent, and convection is less well developed. Further, the influences of the absorption of direct solar radiation and of the diurnal variation of K seem to be insignificant in winter, the insignificance of the latter showing again the absence of strong convection.

Finally, in Section 9, some more general conclusions drawn from this investigation are discussed, such as the pronounced differences in the characteristics of the temperature waves over land and over the oceans, especially when the sea is in a turbulent condition (because it then gives rise to a much larger effective heat capacity). Further, it is suggested that when a strong, unstable thermal boundary layer is present, the virtual diffusivity coefficient K depends not only on the local stability $\partial\theta/\partial z$, but also on its integrated value, from the surface up to the level where the potential temperature is nearly equal to the surface value θ_s. That is to say, in a more complete theory, the appropriate stability parameter should include the potential temperature differences $\Delta\theta_1=\theta_s-\theta_m$ and $\Delta\theta_2=\theta-\theta_m$, as well as the rate of heat input, where θ_s, θ_m and θ are the potential temperature at the surface, the minimum potential temperature at some mid-level, and the ambient potential temperature at the height under consideration, respectively.

2. General features of the diurnal temperature waves

To illustrate the nature of the diurnal temperature waves near the earth's surface during a clear summer day, we present in Figs. 1a–f a set of individual and average observations made by the Great Plains turbulence field project at O'Neill, Nebr., during the summer of 1953 (Lettau and Davidson, 1957). The daily trends are removed in order to reveal more prominently the nature of the pure diurnal temperature waves. The average temperature changes at various depths in the ground based on all of the six complete periods of observation are plotted in Fig. 1a. The normal features of the temperature wave propagation by conduction are clearly shown; namely, the attenuation of amplitude and the increase of phase with distance from the surface. The large temperature gradient during the day as compared to that during the night is a clear indication of the dominance of the daytime surface heating. We note that the vertical temperature gradient in the first 6 cm of the ground reverses itself about 2 hr after sunrise and again about 1 hr before sunset.

These regular features indicate that the diurnal temperature wave in the ground is governed essentially by the classical heat conduction equation. The influence of the variation of the thermal diffusivity with depth and with time of the day, caused by the variation of the moisture content of the soil, appears not to be great, except probably within the topmost few millimeters, even though it may be of some importance for the details of the heat flow in soil.

The corresponding average diurnal temperature variations at various elevations in the atmosphere, also with their daily trends removed, are illustrated in Fig. 1b. These temperature variation curves also show the normal reduction of amplitude as well as increase of phase of the temperature wave with height, and the reversal of the vertical temperature gradient after sunrise and before sunset. However, here the changes take place very rapidly within a relatively thin boundary layer, whose depth is on the order of only a few meters, while above this layer the amplitude and phase change very slowly. This is especially so for the phase e_m of the temperature maxima, which appears to be increasing only slightly from a few meters to a few hundred meters above the surface in the atmosphere, in contrast to the almost linear increase of e_m in the ground, as can be seen from the repective dash-dot curves through the highest points of the temperature curves in Figs. 1a and 1b. These various features suggest that above the shallow boundary layer of the atmosphere the vertical transfer of heat during the day is accomplished by thermal convection. This conclusion is clearly substantiated by the temperature variation curves of the fifth observation (24–25 August) in Fig. 1c and the temperature profiles of the sixth observation (31 August–1 September) in Fig. 1d. These observations were over two periods of comparatively smaller stability and stronger convective activity, as can be seen from the upward spread of the adiabatic lapse rate in these graphs. Further, these two periods are relatively free from irregularities such as those caused by the passages of fronts, and they are therefore more representative of the pure diurnal temperature waves than the other observations. Thus, we notice from the temperature profiles in Fig. 1d that at 0835 (0801 local time) convection has already penetrated to the 500-m level on this day, and by 1035 it has destroyed the temperature inversion, which had been built up by the nighttime cooling from below. From then on until late in the afternoon convection controls the temperature variation in the whole lower atmosphere below 1500 m, making this layer nearly adiabatic, except very close to the ground where almost all the unstable, negative gradient of potential temperature is concentrated. This temperature structure is a characteristic feature common to all six individual observations, even though the convective activity seems to be less fully developed during the other periods of observations, which are in general characterized by more stable stratifications. In spite of the differences in the stability and the depth of penetration of convection, the thickness of the thermal boundary layer revealed by all these observations is about 2–3 m. It is within this thin layer that the very rapid changes of amplitude and phase take place, in contrast to the more gradual changes in the ground.

Another distinct feature of the diurnal temperature changes in the atmosphere revealed by these observa-

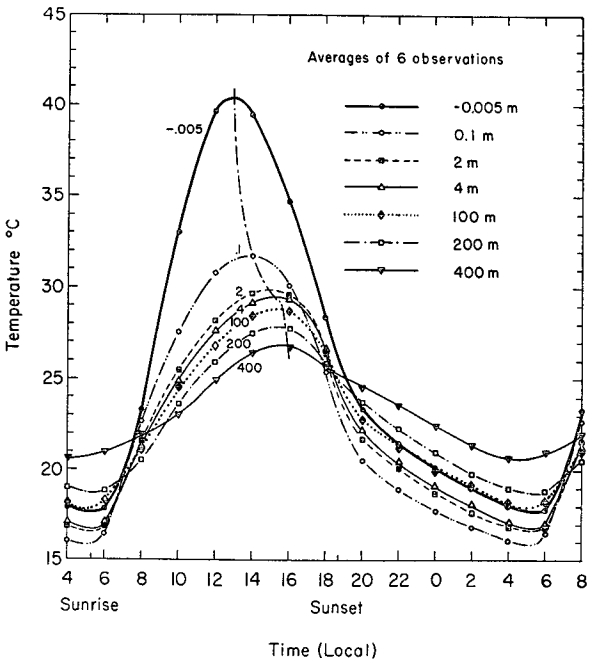

FIG. 1b. Average diurnal temperature variations at various elevations (in meters) in the atmosphere taken at O'Neill, Nebr., summer 1953. The locus of the temperature maxima is represented by the dash-dot curve passing through the highest points of the temperature curves.

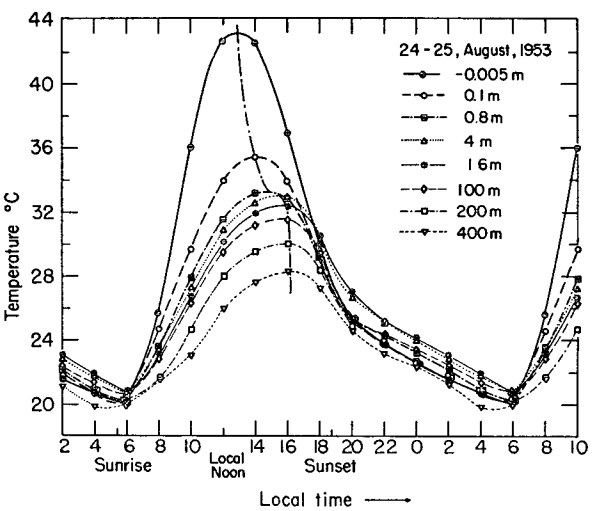

FIG. 1c. Diurnal temperature variations at various elevations during the fifth observation at O'Neill, Nebr.

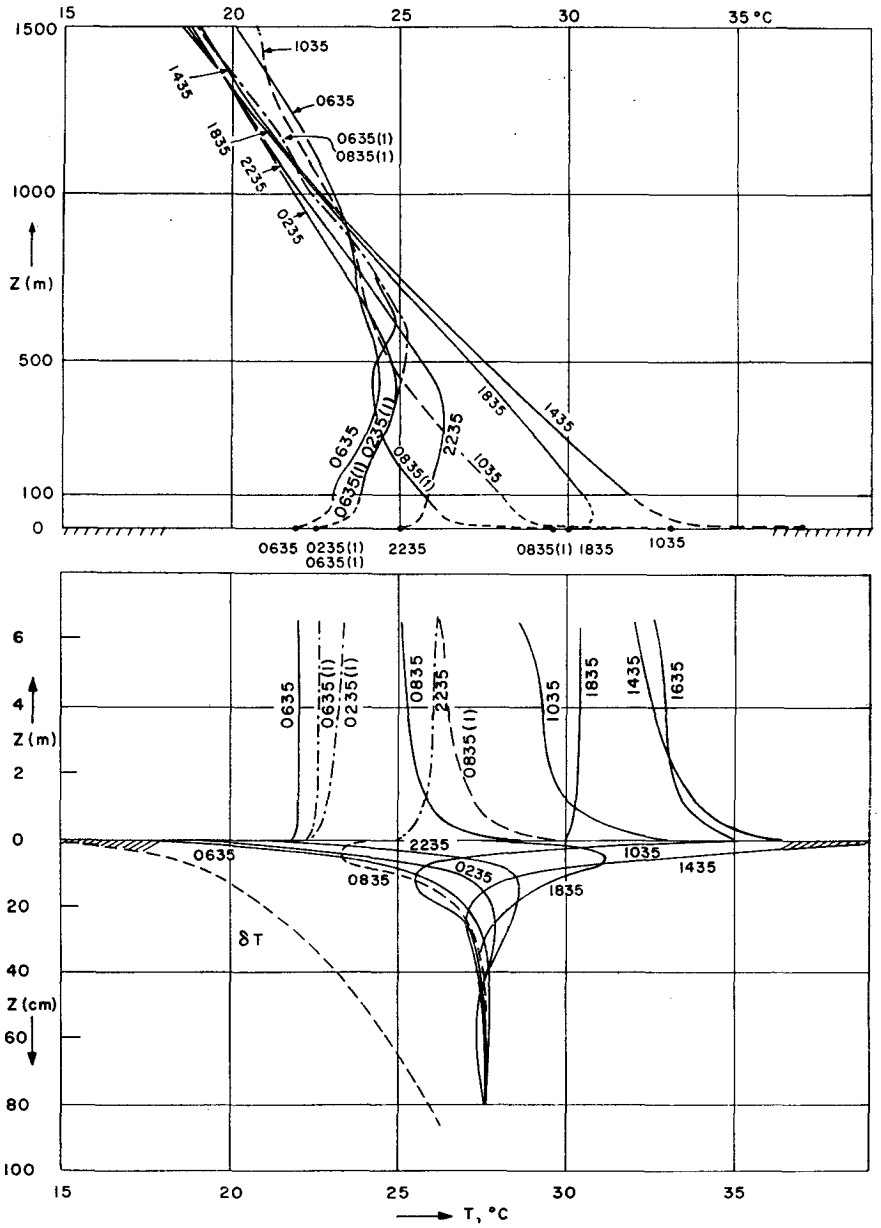

FIG. 1d. Temperature profiles in the air and in the ground during the sixth observation (31 August–1 September 1953) at O'Neill, Nebr. Time on curves represents Central Standard Time. The dashed curve marked as δT in the lower diagram, when shifted by 15C to the left, represents the correction added to the measured soil temperatures to remove a strong mean gradient buildup by the continued heating of the surface layers during the previous few days.

tions is the relative uniformity of the rate of cooling during the night within the first few hundred meters of the atmosphere; this results in the almost constant lapse rate in the atmosphere, and the almost parallel courses of the temperature curves as can be seen from the temperature profiles in Fig. 1e. These profiles, together with those of Fig. 1d, illustrate the contrast between the propagation of the heat waves in the atmosphere and in the ground.

Because of the lack of measurements of the true surface temperature, we shall instead use the temperature T_1 at 0.5 cm below the surface. A representative surface temperature can also be obtained from the temperature profile of the ground by theoretical extrapolation. For ease of comparison with the theoretical results, we have plotted in Fig. 1f the normalized temperature $T_n=(T_1-\bar{T}_1)/\Delta T$, where $\bar{T}_1$ represents the average of the maximum and minimum of T_1, and ΔT their difference.

It is seen that the diurnal variations of T_n are remarkably regular, and the differences between the values for the individual days are relatively small. The temperature close to the surface is seen to rise very rapidly just after sunrise, reaching its maximum at between 1230–1400 local time, and then falling as rapidly in the late afternoon; it then follows a much reduced cooling rate after sunset, reaching its minimum at or slightly after sunrise.

Since the nature of the diurnal temperature wave set up by the solar radiation in the atmosphere is represented clearly by the variations of the relative amplitude A and the phase e_m of the temperature maximum with height, the values of these two quantities are obtained from the observations discussed above and are given in Table 1 for easy reference. The first two lines give the average A and the average e_m for the fifth and the sixth periods of observations (24–25 August and 31 August–1 September), both of which are relatively free of other disturbances, while the last two lines give the average relative amplitude and phase for all the six complete periods of observations. These values indicate very clearly again, as observed in the atmosphere at O'Neill, the boundary-layer nature of the diurnal temperature wave, with A diminishing and e_m increasing

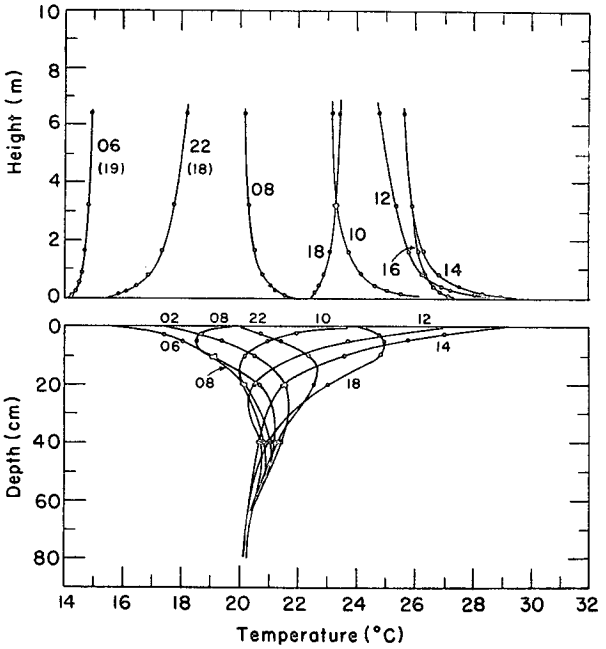

FIG. 1e. Representative temperature profiles in the lowest layer of the atmosphere and in the ground as observed at O'Neill, Nebr., summer 1953. Times are local.

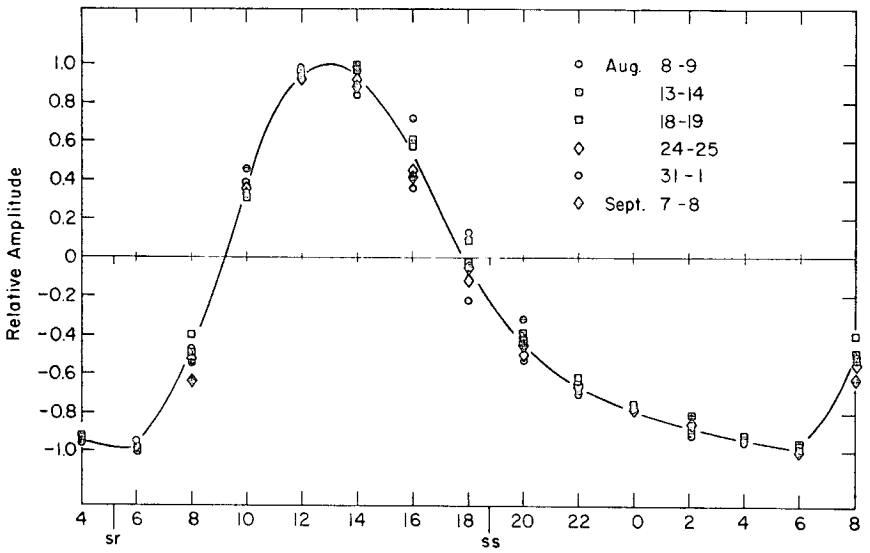

FIG. 1f. Observed variations of the normalized temperatures T_1 and their mean values at O'Neill, Nebr., summer 1953.

TABLE 1. Observed variations with height of the relative amplitude A and phase e_m (local time) of the temperature maximum.

	Height (m)									
	−0.005	0	0.1	2	4	8	16	100	200	400
A (5+6)	0.91	1.0	0.565	0.460	0.432	0.420	0.405	0.380	0.340	0.270
e_m (5+6)	1300	—	1350	1420	1442	1450	1455	1500	1510	1530
A (all)	0.91	1.0	0.640	0.543	0.512	0.500	0.493	0.450	0.360	0.250
e_m (all)	1300	—	1400	1500	1508	1510	1520	1525	1530	1540

very rapidly with height within the first 2–3 m and very slowly above that level. Similar variations are revealed by other observations during the summer when solar radiation is present during a greater part of the day.

Thus, these observations show that the diurnal temperature waves in the lowest layers of the atmosphere during the summer are governed by quite complex physical processes. Our principal aims in this investigation are to uncover these processes, express them mathematically, and construct a simple mathematical model for their representation and prediction.

3. Radiation and turbulent heat conduction equation in the atmosphere, and boundary conditions

We consider the atmosphere as a horizontally stratified medium where all the physical variables are functions of the height z only. In the absence of transport by the mean motion and with no condensation, the local rate of change of the potential temperature θ may be taken as

$$\rho c_p\frac{\partial\theta}{\partial t}=\frac{\partial}{\partial z}\left[\rho c_p K_t\frac{\partial\theta}{\partial z}\right]+(P/p)^n\frac{\partial}{\partial z}\left[S\cos u-\sum_j(A_j-B_j)\right]$$

$$\doteq\frac{\partial}{\partial z}\left[\rho c_p K_t\frac{\partial\theta}{\partial z}+S\cos u-\sum_j(A_j-B_j)\right], \tag{3.1}$$

where ρ is the density, c_p the specific heat under constant pressure, K_t the turbulent thermal diffusivity (assumed to include the effect of thermal convection), p pressure, P its surface value, $n=R/c_p=2/7$, S is the intensity of solar radiation, u the solar zenith angle, and A_j and B_j are the angle-averaged (Eddington's approximation) net upward and downward fluxes of terrestrial radiation in the wavelength interval $\Delta\lambda_j$ of the absorption band centered at the wavelength λ_j, the summation being over the whole spectrum.

Since we are concerned in this investigation only with the temperature changes within the first few hundred meters of the atmosphere, we may replace the factor $(P/p)^n$ by unity without committing any appreciable error. The density ρ is also treated as constant in the following developments for the same reason.

The quantities A_j, B_j and S are governed by the following Schwarzschild radiative transfer equations (see Goody, 1964):

$$\frac{dA_j}{dz}=-k_j(A_j-E_j), \tag{3.2a}$$

$$\frac{dB_j}{dz}=k_j(B_j-E_j), \tag{3.2b}$$

$$\cos u\frac{dS}{dz}=k'S, \tag{3.2c}$$

where k_j and k' are the atmosphere's effective volume absorption coefficients for longwave radiation at wavelength λ_j and for shortwave solar radiation, respectively, and E_j is the blackbody radiation in the interval $\Delta\lambda_j$. The influence of the diffusive nature of radiation is taken into consideration by using a k_j value about 5/3 times that for parallel beams.

From (3.2a, b) we find that the net upward flux, $F_j=A_j-B_j$ for $\Delta\lambda_j$, satisfies the equation

$$\frac{d^2F_j}{dz^2}-k_j^2F_j=2k_j\frac{dE_j}{dz}. \tag{3.2d}$$

It is well known that the atmosphere's absorption is highly selective, i.e., is highly wavelength dependent. To take into consideration the influence of the selective absorption of the terrestrial radiation for the problem of the diurnal temperature waves in a simple manner, we divide the atmospheric radiation spectrum into two different groups of regions on the basis of the absorption coefficient and the local scale of variation; namely, a "strongly absorbed" group which includes all those regions or absorption lines of the spectrum with k_λ greater than the local scale of variation d/dz; and a "weakly absorbed" group which includes all those regions with $k_\lambda<d/dz$. Further, we introduce the average fluxes F_s, E_s, F_w and E_w, and the mean absorption coefficients k_s and k_w for these two groups, defined, respectively, by

$$\left.\begin{aligned}F_{s,w}&=\int_{s,w}F_\lambda d\lambda,\quad E_{s,w}=\int_{s,w}E_\lambda d\lambda\\ k_{s,w}&=\frac{\int_{s,w}k_\lambda F_{s,w}d\lambda}{F_{s,w}}=\frac{\int_{s,w}k_\lambda E_\lambda d\lambda}{E_{s,w}}\end{aligned}\right\}, \tag{3.2e}$$

where the subscripts s on the letters and on the integrals refer to quantities of the strongly absorbed regions while the subscripts w are for the weak regions. Notice that the mean absorption coefficients k_s defined above is equivalent to Planck means for the strong lines and k_w is equivalent to the Rosseland mean over the weak lines (see Goody, 1964, p. 58 and Chap. 9).

Eq. (3.2d) may be assumed to hold for the integrals over the two groups; namely,

$$\frac{d^2F_s}{dz^2}-k_s^2F_s=2k_s\frac{dE_s}{dz}=8\gamma K_s\sigma T^3\frac{dT}{dz}, \tag{3.3a}$$

$$\frac{d^2F_w}{dz^2}-k_w^2F_w=2k_w\frac{dE_w}{dz}=8(1-\gamma)k_w\sigma T^3\frac{dT}{dz}, \tag{3.3b}$$

where σ is the Stefan-Boltzman constant, and γ the fraction of the blackbody radiation contained in the

strongly absorbed parts of the spectrum, so that we have $E_s=\gamma\sigma T^4, E_w=(1-\gamma)\sigma T^4$.

If F_s and F_w are eliminated from Eqs. (3.1) and (3.3a, b), there will then result an equation of sixth order in z. On the other hand, if a grey model is used instead of the selective absorption model developed above, only one of the two equations (3.3a, b) will be in existence and the resulting equation will be of the fourth order in z. Such an equation has been obtained by Kibel (1943) and also by Goody (1960).

Instead of using (3.3a, b) directly, we shall now assume the following extreme conditions to be valid for the two groups of spectral regions; namely, $k_s \gg d/dz$ and $k_w \ll d/dz$, respectively. Under these conditions the two equations above may be simplified to

$$F_s = -\rho c_p K_r \frac{dT}{dz}, \tag{3.4a}$$

$$\frac{d^2F_w}{dz^2} = \rho c_p a^2 \frac{dT}{dz}, \tag{3.4b}$$

where K_r and a^2 are given by

$$K_r = \frac{8\gamma\sigma T^3}{\rho c_p k_s}, \quad a^2 = \frac{8(1-\gamma)\sigma T^3}{\rho c_p} k_w. \tag{3.4c}$$

Eq. (3.4 b) may be integrated once to give

$$\frac{1}{\rho c_p}\frac{dF_w}{dz} = a^2(T-\bar{T}) \doteq a^2(\theta-\bar{\theta}), \tag{3.4b'}$$

where $\bar{T}$ is a reference temperature. Here the difference between T and θ may be neglected and the factor T^3 in K_r and a^2 may be treated as constant.

Substituting F_s and F_w from (3.4a) and (3.4b) into (3.1), we obtain

$$\frac{\partial\theta}{\partial t} = \frac{\partial}{\partial z}\left\{K\frac{\partial\theta}{\partial z} + \left(\frac{\cos u}{\rho c_p}\right)S\right\} - a^2(\theta-\bar{\theta}), \tag{3.5}$$

where $K=K_t+K_r$ is the virtual conductivity. This equation shows that the influence of the flux of terrestrial radiation due to the strongly absorbed parts of the spectrum is the same as diffusion while that due to the weakly absorbed parts of the spectrum results in a Newtonian cooling.

It may be pointed out, since the classification of the spectral regions is with reference to the local scale of variation, that the relative importance of the two parts of the spectrum depends upon the location and therefore upon the specific problem under consideration. Thus, when applied to the present problem of the temperature wave in the surface boundary layer, we must use as the criterion for classification the rate of change of the amplitude of the temperature wave near the surface, which measures the sensible heat transfer and which is determined by the intensity and the duration of the solar radiation. According to the observed amplitude variations near earth's surface presented in the preceding section, the diurnal heat wave during a hot summer day may be represented by $d/dz \simeq 10^{-3}-10^{-2}$ cm^{-1}, while $k_s=\rho_w k_{ms} < 10^{-4}$ cm^{-1} for a normal surface vapor density $\rho_w=8$ gm m^{-3}. Hence, for these cases the scale length dz is much smaller than the photon mean free path k^{-1} for the whole range of the water vapor spectrum, which corresponds to a vanishingly small γ. Thus, under these circumstances the influence of the flux of terrestrial radiation in the surface boundary layer is a pure Newtonian cooling. On the other hand, for the mean temperature distribution and under conditions when no intense thermal boundary layer is in existence we have $d/dz < 10^{-5}$ cm^{-1}, which is smaller than the k_s values of the strongly absorbed regions of the water vapor spectrum. Thus, by taking $\sigma=1.37\times10^{-12}$ cal cm^{-2} sec^{-1} (°C)$^{-4}$, $\gamma_0=0.5$, $\rho c_p=3\times10^{-4}$ cal cm^{-3} (°C)$^{-1}$, $T=280$K, $k_s=10^{-4}$ cm^{-1}, $k_w=5\times10^{-6}$ cm^{-1}, we find for the mean temperature distribution

$$K_{r0}=4\times10^3 \text{ cm}^2 \text{ sec}^{-1}, \quad a^2=2\times10^{-6} \text{ sec}^{-1};$$

while for the diurnal temperature wave during a hot summer day when an intense thermal boundary layer is present, we have

$$K_r=0, \quad a^2=4\times10^{-6} \text{ sec}^{-1}.$$

The appropriate value of K_r for winter or a cool summer day when no intense thermal boundary layer is present is most probably somewhere between the two values cited above.

It is apparent that a fairly large radiative diffusivity must also be active on a turbulent ocean surface where most of the solar radiation will be transferred downward and, hence, no thermal boundary layer can exist. It may be remarked that if, instead of the two-group selective absorption model used above, we use a grey model as in Kibel's (1943) and Goody's (1964) treatments of the problem, then the opaque approximations $k \gg d/dz$ will lead to pure radiative diffusion while the transparent approximation $k \ll d/dz$ will result in pure Newtonian cooling, but not both simultaneously as is the case in the present model. A fuller development of this new model and its application to other problems will be presented in another paper (Kuo, 1968).

For the investigation of the diurnal temperature changes it is convenient to represent θ and the other quantities by Fourier series in time, i.e.,

$$\theta(z,t) = \sum_{n=0}^{\infty} \theta_n^{(c)} \cos nqt + \theta_n^{(s)} \sin nqt,$$

$$= \sum_{n=-\infty}^{\infty} \theta_n(z) e^{-inqt}, \tag{3.6a}$$

$$\frac{\cos u}{\rho c_p}\frac{\partial S}{\partial z}=\sum_{n=0}^{\infty} T_{sn}(z)\cos nqt, \tag{3.6b}$$

$$K(z,t)=\bar{K}(z)+\sum_{n=1}^{\infty} A_n{}^{(c)}\cos nqt,$$

$$=\bar{K}(z)+\tfrac{1}{2}\sum_{m=-\infty}^{\infty} A_m{}^{(c)}e^{-imqt}, \tag{3.6c}$$

where $\bar{K}$ is the time average of K and $\theta_n(z)=\theta_n{}^{(r)}+i\theta_n{}^{(i)}$ is the complex amplitude satisfying the relations

$$\left.\begin{aligned}&\theta_n{}^{(r)}=\theta_{-n}{}^{(r)}=\tfrac{1}{2}\theta_n{}^{(c)}\\ &\theta_n{}^{(i)}=-\theta_{-n}{}^{(i)}=\tfrac{1}{2}\theta_n{}^{(s)},\quad A_m{}^{(c)}=A_{-m}{}^{(c)}\end{aligned}\right\}. \tag{3.6d}$$

Substituting these expansions in (3.5), we then obtain the following spectral equations for the mean potential temperature θ_0 and for the various higher harmonics ($n\geqslant 1$):

$$\frac{\partial}{\partial z}\left(\bar{K}_0\frac{\partial\theta_0}{\partial z}\right)-a^2(\theta_0-\bar{\theta})=-\frac{1}{\rho c_p}\frac{\partial}{\partial z}(S\cos u)_0$$

$$-\tfrac{1}{4}\sum_{n=1}^{\infty}\frac{\partial}{\partial z}\left[A_n{}^{(c)}\frac{\partial\theta_n{}^{(r)}}{\partial z}\right], \tag{3.7}$$

$$\frac{\partial}{\partial z}\left(\bar{K}\frac{\partial\theta_n}{\partial z}\right)+(nqi-a^2)\theta_n=-\frac{1}{\rho c_p}\left(\frac{\partial S}{\partial z}\cos u\right)_n$$

$$-\sum_{m=1}^{\infty}\frac{\partial}{\partial z}\left(A_m\frac{\partial\theta_{n-m}}{\partial z}\right), \tag{3.8}$$

where K_0 and $\bar{K}$ are the time averages of the virtual conductivities for θ_0 and θ_n, respectively, including the appropriate contributions from longwave radiation.

We notice that in this new formulation of the problem, a "time-eddy transport" term

$$-K'\frac{\partial\theta'}{\partial z}=-\tfrac{1}{4}\sum_{n=1}^{\infty}A_n{}^{(c)}\frac{\partial\theta_n{}^{(r)}}{\partial z},$$

representing the correlation between the instantaneous values of K' and $-\partial\theta'/\partial z$ appears in the mean heat transfer equation. Since K is large on account of the convective activity during the day when $\partial\theta/\partial z$ is negative, this term gives rise to a large upward transport of heat on the average. Hence, the inclusion of this "eddy" term removes the one long-standing difficulty that the transfer of heat by turbulence when expressed in terms of $\partial\theta/\partial z$ represents a downward transport. Notice further that the time-variable part of K also creates higher harmonics in (3.8).

The first term on the right-hand side of (3.8) can be obtained either from the solution of (3.2b), or from known empirical formulae, such as those derived by Mügge and Möller (1932) and by McDonald (1960), for the absorption of solar radiation F_{as} by the vapor content of the atmosphere; namely,

$$F_{as}=b(x\sec u)^{0.3}, \tag{3.9}$$

where

$$x=\int_z^{\infty}(p/p_0)\rho_w dz$$

is the effective water vapor content of the column of atmosphere of unit cross-sectional area above z; b is a constant equal to 0.149 cal min^{-1} gm$^{-0.3}$ cm$^{-1.4}$ according to McDonald, while Mügge and Möller give $b=0.172$. The corresponding heating rate produced by F_{as} is given by

$$\frac{\partial T_{as}}{\partial t}=-\frac{\cos u}{\rho c_p}\frac{\partial F_{as}}{\partial z}=\left(\frac{0.3bp}{c_p p_0}\right)\left(\frac{\rho_w}{\rho}\right)\left(\frac{\cos u}{x}\right)^{0.7}. \tag{3.9a}$$

Here the average value of the factor $x^{-0.7}$ increases slightly with height while the product of the mixing ratio ρ_w/ρ and p/p_0 usually decreases with height; hence, the average value of $\partial T_{as}/\partial t$ changes only slightly with height within a deep layer of the troposphere, and the coefficient of $(\cos u)^{0.7}$ may therefore be taken as a constant.

The solar radiation term $S\cos u$ is given by

$$\left.\begin{aligned}S\cos u&=S\cos\varphi\cos\delta\,(\cos qt-\cos H),\quad \text{for } 0\leqslant|qt|\leqslant H\\ &=0,\quad \text{for } H\leqslant|qt|\leqslant\pi\end{aligned}\right\} \tag{3.10}$$

where t is measured from the solar noon, $q=7.292\times10^{-5}$ sec^{-1}, $t_0=12H/\pi$ is the hour angle of sunset, $\cos H=-\tan\delta\tan\varphi$, φ is the latitude and δ is the solar declination.

For our solution we expand $(\cos qt-\cos H)$ and its 0.7th power into Fourier series. Thus,

$$\{\cos qt-\cos H,\,0\}=\sum_{n=0}^{\infty}b_n\cos nqt, \tag{3.11}$$

$$\{(\cos qt-\cos H)^{0.7},\,0\}=\sum_{n=0}^{\infty}b_n'\cos nqt, \tag{3.12}$$

where the zero values of the functions during the night are taken into consideration. The coefficients b_n can be determined analytically for any arbitrary H and are given by

$$b_0=\frac{1}{\pi}(\sin H-H\cos H), \tag{3.11a}$$

$$b_1=\frac{1}{\pi}(H-\sin H\cos H), \tag{3.11b}$$

$$b_n=\frac{2\,(\sin nH\cos H-n\cos nH\sin H)}{\pi\qquad n(n^2-1)},\quad \text{for } n>1. \tag{3.11c}$$

At the equinox, i.e., for $H=\pi/2$, the expressions (3.11b,

TABLE 2. Values of b_n' for 1. $H=\pi/2$ and 2. $H=13\pi/24$ for values of n from 1–7.

	1	2	3	4	5	6	7
1.	0.53166	0.18554	−0.04302	−0.05346	0.01722	0.02788	−0.00094
2.	0.59562	0.16100	−0.06956	−0.03252	0.03750	0.01286	−0.02140

c) simplify to

$$b_1=\tfrac{1}{2}, \tag{3.11b'}$$

$$\left.\begin{aligned} b_n&=\frac{2(-1)^{m+1}}{\pi(4m^2-1)}, \quad \text{for } n=2m>0\\ &=0, \quad \text{for } n=2m+1 \end{aligned}\right\}. \tag{3.11c'}$$

The coefficients b_n' of (3.12) can be obtained numerically, and their values for $H=\pi/2$ and $H=13\pi/24$ are given in Table 2. Thus, the temperature change (°C) produced by the direct absorption of solar radiation may be written as

$$T_{as}=B\sum_{n=1}^{\infty}\frac{b_n'}{n}\sin nqt, \tag{3.13}$$

where

$$B=\frac{0.3b\rho_w}{q\rho c_p}\left(\frac{\cos\varphi\cos\delta}{x}\right)^{0.7}.$$

Assuming that radiative processes and evaporation are absent in the ground,[1] the nth harmonic of the ground temperature departure T_e' satisfies the familiar homogeneous conduction equation with a thermal conductivity K_e, i.e.,

$$\frac{\partial T_{en}'}{\partial t}=\frac{\partial}{\partial z}\left(K_e\frac{\partial T_{en}'}{\partial z}\right). \tag{3.14}$$

Our problem is to determine θ' and T_e' as functions of t and z from the two conduction equations (3.8) and (3.14) and the appropriate boundary conditions, which we shall derive presently. Since the changes of θ' and T_e' are considered as the results of the heat exchanges at the ground surface, both of them must be finite at great distances from the ground. Hence, we have

$$\theta' \text{ finite as } z\to\infty \text{ and } T_{en}' \text{ finite as } z\to-\infty. \tag{3.15a}$$

At the surface the temperature must be continuous, and the algebraic sum of the various heat fluxes must vanish. Further, we shall assume that the earth's surface radiates as a blackbody but it reflects a fraction r_1 of the solar radiation and a fraction r_2 of the longwave radiation that falls on it. Then the two surface conditions mentioned above may be written as

$$\theta'=T_e', \tag{3.15b}$$

$$\rho c_p K\frac{\partial\theta'}{\partial z}-\rho_e cK_e\frac{\partial T_e'}{\partial z}+S_1-G+R-E=0, \tag{3.15c}$$

where S_1 is the surface net downward flux of solar energy, G the upward flux of longwave radiation from the ground, R the downward flux of atmospheric radiation, and E the upward flux of latent heat of evaporation.

In this work we shall not calculate E separately, but consider it included in the first term by introducing the Bowen ratio $1/m$, that is, the ratio of sensible to latent heat flux, and by replacing ρ by $\bar{\rho}=\rho(1+m)$. The upward radiation G from the earth may be taken simply as a blackbody radiation at the surface temperature T_s, i.e., $G=\sigma T_s^4$. On the other hand, the atmospheric back-radiation R is rather complicated as it depends both on the temperature and the humidity distributions in the lower layers of the atmosphere. However, the success of Angström's or Brunt's (1939) empirical formula indicates that it can be taken as approximately equal to a fraction b^* of the surface blackbody radiation, with b^* depending on the moisture content of the air. Alternatively, we may take R as approximately given by the blackbody radiation at a certain effective temperature T_1; namely, $R=\sigma T_1^4$, with T_1 depending on the moisture content. For the present problem of periodic temperature waves, the value of T_1 can be determined by the heat-balance requirement. Thus, the nocturnal radiation $R_n=G-R$ may be written as

$$R_n=\sigma(T_s^4-T_1^4)=h(T_s-T_1)=hT_s'+h(\bar{T}_s-T_1), \tag{3.16}$$

where $h=\sigma(T_s^2+T_1^2)(T_s+T_1)=4\sigma\bar{T}^3$, $\bar{T}_s$ is the mean surface temperature, T_s' the departure of the surface temperature from this mean, and $\bar{T}$ the average value of T_s and T_1.

As for the downward flux of solar energy S_1 at the surface, we observe that, besides absorption, the atmosphere and the ground surface also reflect part of the solar radiation into space. Hence, the amount of the solar energy absorbed by a unit area of the surface during the day may be taken as approximately given by

$$\begin{aligned} S_1&=\gamma^*\cos u(I_0-F_{as0}),\\ &=S_0\sum_{n=1}^{\infty}\bar{b}_n\cos nqt, \end{aligned} \tag{3.17}$$

where I_0 is the solar constant, $(1-\gamma^*)$ the effective albedo of the earth-atmosphere system, F_{as0} the surface value of F_{as}, which is given by (3.9), $S_0=I_0\cos\varphi\cos\delta$, $b_n=\bar{b}_n-B_1b_n'$, $B_1=b[x_0/(\cos\varphi\cos\delta)]^{0.3}/I_0$, and b_n and b_n' are given by (3.11a–d) and in Table 2.

[1] Circumstances exist where it may be necessary to include these two processes in Eq. (3.14).

Thus, the total downward radiative flux at the surface may be written as

$$F=-hT_s'+S_0\sum_{n=1}^{\infty}\bar{b}_n\cos nqt+S_0\bar{b}_0-h(\bar{T}_s-T_1). \quad (3.18)$$

Since in this study we are concerned with the periodic diurnal temperature variations only, we shall equate $S_0\bar{b}_0$ with the average rate of heat loss by longwave radiation, viz., $h(\bar{T}_s-T_1)$. In this case the equation above reduces to

$$F=-hT_s'+S_0\sum_{n=1}^{\infty}\bar{b}_n\cos nqt. \quad (3.18')$$

Substituting these expansions in the boundary conditions (3.15b, c), we then obtain for $z=0$

$$\theta_n=T_n, \quad (3.18a)$$

$$-\bar{\rho}c_p\left[\bar{K}\frac{d\theta_n}{dz}+A_n\frac{d\theta_0}{dz}+\tfrac{1}{2}\sum_{m=1}^{\infty}A_m\frac{d\theta_{n-m}}{dz}\right]+\rho_e cK_e\frac{dT_n}{dz}+hT_n=S_0\bar{b}_n. \quad (3.18b)$$

4. Solutions for constant diffusivities and the influences of longwave and direct solar radiation.

Even though the virtual thermal diffusivity K of the atmosphere is far from being constant, a discussion of the solutions of the conduction equations for the two media with constant diffusivities and the boundary conditions [Eqs. (3.18a, b)] will reveal many important and interesting features of this problem and help us to understand the situation better when the influences of the variations of K are taken into consideration. Hence, we shall investigate this simple problem first.

On taking into consideration the influence of the absorption of direct solar radiation given by (3.13), it is readily found from (3.8) that the total solution for the diurnal temperature wave may be written as

$$\theta'=\sum_{n=1}^{\infty}\left\{\theta_{n0}\exp(-k_{1,n}\zeta_n)\cos(nqt-e_n-k_{2,n}\zeta_n)+\frac{Bb_n'}{n}\sin nqt\right\}, \quad (4.1)$$

where B and b_n' are defined in (3.13), and

$$\left.\begin{aligned}\zeta_n&=(nq/2K)^{\frac{1}{2}}z\\ k_{1,n}^2&=(1+a^4/n^2q^2)^{\frac{1}{2}}+a^2/nq\\ k_{2,n}^2&=(1+a^4/n^2q^2)^{\frac{1}{2}}-a^2/nq\end{aligned}\right\}, \quad (4.1a)$$

and a^2 is the Newtonian cooling factor given by (3.4c). Here the first sum represents the solution of the homogeneous equation and θ_{n0} and e_n are as yet unspecified constants, to be determined by the boundary conditions.

From the expressions of $k_{1,n}$ and $k_{2,n}$ we conclude that the effect of the Newtonian cooling term of (3.8) is to increase the attenuation rate and to reduce the change of phase with height. However, on making use of the normal value $a^2=4\times10^{-6}$ sec^{-1} obtained in the preceding section, we then find $(a^2/nq)<0.055$, and hence the effect of the Newtonian cooling on the diurnal heat wave in the atmosphere is quite small and may therefore be neglected. On the other hand, this influence is of importance for the determination of the mean temperature distribution. Thus, in what follows we shall set a^2 equal to zero in (3.8), but retain the $a_0^2(\theta_0-\bar{\theta})$ term in (3.7).

From (4.1) we find that the conductive heat flux at the surface is given by

$$f_0=-\bar{\rho}c_pK\left(\frac{\partial\theta'}{\partial z}\right)_{z=0}=\sum_{n=1}^{\infty}\lambda_n\theta_{n0}[\cos nqt(\cos e_n+\sin e_n)+\sin nqt(\sin e_n-\cos e_n)], \quad (4.2)$$

where

$$\lambda_n=\bar{\rho}c_p\left(\frac{nq}{2}K\right)^{\frac{1}{2}}.$$

The corresponding solutions T' and $f_0'=[\rho_e cK_e(\partial T'/\partial z)]_{z=0}$ for the lower medium with constant K_e are given by, respectively,

$$T'=\sum_{n=1}^{\infty}T_{n0}\exp(\zeta_n')\cos(nqt-e_n'+\zeta_n'), \quad (4.3a)$$

$$f_0'=\sum_{n=1}^{\infty}\lambda_{en}T_{n0}[\cos nqt(\cos e_n'+\sin e_n')+\sin nqt(\sin e_n'-\cos e_n')], \quad (4.3b)$$

where $\zeta_n'=(nq/2K_e)^{\frac{1}{2}}z$ and $\lambda_{en}=\rho_e c(nqK_e/2)^{\frac{1}{2}}$.

On substituting these solutions into the surface conditions (3.18a, b) and equating to zero the coefficients of $\cos nqt$ and $\sin nqt$ separately, we obtain

$$T_{n0}\cos e_n'=\theta_{n0}\cos e_n, \quad (4.4a)$$

$$T_{n0}\sin e_n'=\theta_{n0}\sin e_n+\frac{Bb_n'}{n}, \quad (4.4b)$$

$$(\lambda_{en}+h)T_{n0}\cos e_n'+T_{n0}\lambda_{en}\sin e_n'+\lambda_n\theta_{n0}(\cos e_n+\sin e_n)=S_0\bar{b}_n, \quad (4.4c)$$

$$T_{n0}[(\lambda_{en}+h)\sin e_n'-\lambda_{en}\cos e_n']+\lambda_n\theta_{n0}[\sin e_n-\cos e_n]=0. \quad (4.4d)$$

Dividing (4.4b) by (4.4a), we obtain

$$\tan e_n' = \tan e_n + \frac{Bb_n'}{n\theta_{n0}} \frac{1}{\cos e_n}, \tag{4.5}$$

and on substituting $T_{n0}\cos e_n'$ and $T_{n0}\sin e_n'$ from (4.4a, b) in (4.4d), we find

$$\tan e_n = \frac{(\lambda_{en}+\lambda_n)}{(\lambda_{en}+\lambda_n+h)} - \frac{(\lambda_{en}+h)Bb_n'}{(\lambda_{en}+\lambda_n+h)n\theta_{n0}\cos e_n}. \tag{4.6}$$

Similarly, substituting $T_{n0}\cos e_n'$ and $T_{n0}\sin e_n'$ from (4.4a, b) in (4.4c) and making use of (4.6), we obtain

$$\theta_{n0} = \frac{S_0 b_n \cos e_n}{(\lambda_{en}+\lambda_n+h)} \times\{1-B_n'[\lambda_{en}+(\lambda_{en}+h)\tan e_n]\}, \tag{4.7}$$

where $B_n' = Bb_n'/(S_0 b_n n)$, with dimensions in (°C) cm^2 sec cal^{-1}, the inverse of the dimensions of λ_n. Setting θ_{n0} from (4.7) in (4.6), we then obtain

$$\tan e_n = \frac{(1-B_n'\lambda_{en})\tan e_{n0} - B_n'(\lambda_{en}+h)}{1-B_n'[\lambda_{en}-(\lambda_{en}+h)\tan e_{n0}]}, \tag{4.8}$$

where e_{n0} is the value of e_n when B_n' is absent and is given by

$$\tan e_{n0} = \frac{\lambda_n+\lambda_{en}}{\lambda_n+\lambda_{en}+h}. \tag{4.8a}$$

Thus, Eq. (4.8) determines e_n in terms of the physical parameters λ_n, λ_{en}, h and B_n', while (4.7) determines θ_{n0}.

It is readily seen from (4.8) that when $B_n'=0$ (i.e., when there is no absorption of solar radiation in the atmosphere), we then have

$$e_n = e_n' = \tan^{-1}\left(\frac{\lambda_n+\lambda_{en}}{\lambda_n+\lambda_{en}+h}\right) = e_{n0}, \tag{4.9}$$

$$\theta_{n0} = \frac{S_0 b_n \cos e_n}{\lambda_n+\lambda_{en}+h}. \tag{4.10}$$

Further, if the surface longwave radiation factor h is also set to zero, we then find

$$e_n = \frac{\pi}{4}, \tag{4.9a}$$

$$\theta_{n0} = \frac{S_0 b_n}{2(\lambda_{en}+\lambda_n)}, \tag{4.10a}$$

expressions which agree with the results obtained by Brunt (1932) and by Jaeger and Johnson (1953).

Eqs. (4.2), (4.3b) and (4.10) show that the surface fluxes f_n and f_n' are directly proportional to the values of the parameters λ_n and λ_{en}, respectively, and inversely proportional to the sum $\lambda_n+\lambda_{en}+h$, while (4.10) shows that the amplitude of the surface temperature wave is inversely proportional to $\lambda_n+\lambda_{en}+h$. Hence, the two parameters λ_n and λ_{en} may be called the effective heat capacity of the two media and h represents the effective heat capacity of the space with respect to the surface insolation. According to the relations (4.9) and 4.10), the radiational cooling at the surface tends to reduce the phase lag e_n and the amplitude θ_{n0} in comparison with (4.9a) and (4.10a).

In order to familiarize ourselves with the influences of the various physical parameters on the surface heat wave we make use of the following typical values: $K=3\times10^3$ cm^2 sec^{-1}, $\rho c_p=3\times10^{-4}$ cal cm^{-3} (°C)$^{-1}$, $K_e=2.8\times10^{-3}$ cm^2 sec^{-1}, $\rho_e c=0.36$ cal cm^{-3} (°C)$^{-1}$. Using $q=7.292\times10^{-5}$ sec^{-1}, we then find $\lambda_1=0.992\times10^{-4}$ and $\lambda_e=1.149\times10^{-4}$ cal cm^{-2} sec^{-1} (°C)$^{-1}$, so that the two effective heat capacities are of the same order of magnitude; therefore, the incoming solar energy is being almost equally partitioned at the surface, according to the simple relation (4.10a).

On making use of (4.9a) and (4.10a) and assuming equinox conditions, we find that the diurnal temperature variation at the surface is given by the curve a in Fig. 2, according to which the maximum surface temperature occurs at about 1430 instead of the normally observed occurrence at or before 1300.

To estimate the influence of the surface radiation factor h, we take $\bar{T}=270$K in (3.16) and find $h=1.07786\times10^{-4}$ cal cm^{-2} sec^{-1} (°C)$^{-1}$, so that it is of the same order of magnitude as λ_1 and λ_{e1} cited above. On including this factor in the solution by using the relations (4.9) and (4.10), we find that the diurnal variation of the surface temperature is represented by the curve b in Fig. 2. It is seen that the inclusion of h makes the maximum temperature occur about 40 min earlier than without. Further, it also makes the temperature drop faster during the afternoon and slower during the night, in addition to a reduction of the amplitude. Thus,

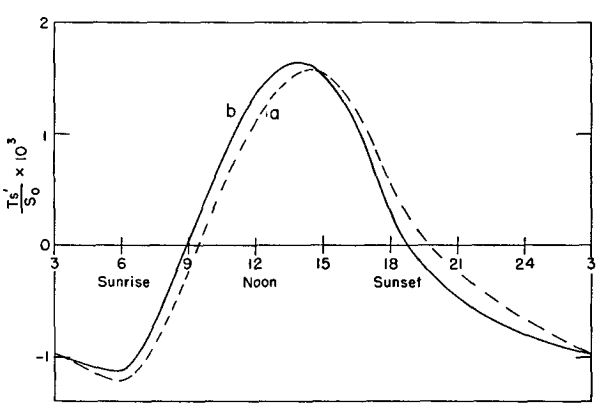

FIG. 2. Diurnal variations of the surface temperature from classical theories with constant thermal diffusivities: a., no heat loss by longwave radiation; b., with radiational exchange.

h appears to be an important factor and must be included in any realistic approach to the diurnal heat problem.

As to the influence of the solar heating factor Bb' in (4.1), it is found that it tends to delay the surface temperature wave a little and to make it drop somewhat faster during the night. Since this influence is more pronounced in the air above than at the ground, we shall discuss it more fully in Section 8.

5. Influence of the vertical variation of $\bar{K}$ in the atmosphere

Since the virtual diffusivity $\bar{K}$ increases by many orders of magnitude from the surface to a few tens of meters above the ground, we must take the vertical variation of $\bar{K}$ into consideration in obtaining the solution of (3.8). However, before endeavoring to obtain the exact solutions of this conduction equation for various variable $\bar{K}$ (as will be done later in this section), let us first examine the qualitative influence of the increase of $\bar{K}$ with height in the boundary layer by making use of an approximate form of the solution. For this purpose we assume that the time-variable part of K is zero (so that $\bar{K}=K$) and write the homogeneous part of (3.8) for a variable K as

$$\frac{\partial^2\theta}{\partial z^2}+g\frac{\partial\theta}{\partial z}=\frac{1}{K}\frac{\partial\theta}{\partial t}, \tag{5.1}$$

where $g=K^{-1}\,dK/dz$ is the logarithmic rate of increase of K with height. This equation shows that a positive g gives rise to heating or cooling according to whether $\partial\theta/\partial z$ is positive or negative.

On treating both g and K as quasi-constants, we may write the solution for the first harmonic as

$$\theta(z,t)=\theta_1 e^{-a_1 z}\cos(qt-bz-e), \tag{5.2}$$

where a_1 and b are given by

$$\left.\begin{aligned} a_1&=\frac{1}{2}(g+p), \quad b=\frac{q}{pK}\\ p^2&=\frac{1}{2}\left[g^2+\left(g^4+\frac{16q^2}{K^2}\right)^{\frac{1}{2}}\right]\end{aligned}\right\}. \tag{5.2a}$$

Since $p>(2q/K)^{\frac{1}{2}}$, a_1 is always greater than and b is always less than $(q/2K)^{\frac{1}{2}}$. Hence, the influence of a positive g is to increase the attenuation rate and to reduce the phase lag of the temperature wave as compared with that for a constant K. Thus, for large g we have $a_1=g$ and $b=q/(dK/dz)$, so that a_1 is proportional to $K^{-1}\,dK/dz$ and b is inversely proportional to dK/dz.

On substituting the solution (5.2) in the boundary conditions (3.18a, b), we find that the surface phase lag e and the amplitude θ_1 of the first harmonic are given by

$$\tan e=\frac{\lambda_e+\lambda' b/a_1}{\lambda_e+\lambda'+h}, \tag{5.3a}$$

$$\theta_1=\frac{S_0\bar{b}_1\cos e}{\lambda_e+\lambda'+h}, \tag{5.3b}$$

where $\lambda'=\bar{\rho}c_pKa_1$. Hence, λ' represents the effective heat capacity of the atmosphere for this case. It can be seen, when $g^2\ll 4q/K$, that λ' approaches the effective heat capacity λ [see equation following (4.2)] for a constant K, whereas for $g^2\gg 4q/K$, we have approximately

$$\lambda'=\bar{\rho}c_p\,dK/dz,$$

so that λ' becomes independent of q and K, and is determined by the vertical gradient of K only. Thus, dK/dz near the surface plays a decisive role in determining the flow of heat into the air and into the ground, and also in determining the phase e of the surface temperature wave. According to (5.3a), e is always less than $\pi/4$ since b/a_1 is always smaller than unity.

It should be remarked that, even though the preliminary information obtained above is very valuable, the solution (5.2) is too crude to be used for comparison with observations when K varies appreciably within the domain of investigation. We shall therefore obtain, in the latter part of this section, the exact solution of the homogeneous part of (3.8) for a variable K. Since, according to Best (1935), there is no single power-law K profile which is representative of all cases, we shall divide the atmosphere into a number of layers and assume a power law distribution of K within each layer. Thus, we set

$$K_j=K_{0j}(z_{j0}\pm z)^p, \tag{5.4}$$

where K_{0j}, z_{j0} and p are the constants of the profile in the jth layer, and use the plus or the minus sign according to whether K_j increases or decreases with height. By proper choice of these constants and with a large number J of layers, any profile of K can be represented very closely.

To find the general diurnal temperature wave solution with this K in the jth layer, we set

$$\theta'(z,t)=\sum_{n=1}^{\infty}\theta_n(z,t)=\sum_{n=1}^{\infty}Q_n(z)e^{-inqt}. \tag{5.5}$$

On substituting this expression in the homogeneous part of (3.8), we find that the amplitude function $Q_n(z)$ of the nth harmonic is given by

$$Q_n(z)=x_n^r\{AJ_r[x_n(1+i)]+BH_r[x_n(1+i)]\}, \tag{5.6}$$

where

$$r=(1-p)/(2-p),$$
$$x_n=[1/(2-p)(2nq/K_{0j})^{\frac{1}{2}}(z_0\pm z)^{1-p/2}],$$

A and B are arbitrary complex constants to be determined by the boundary conditions, and $J_r[x_n(1+i)]$ and $H_r[x(1+i)]$ are the modified Bessel and Hankel functions of order r with complex argument, which can be expressed in terms of the real ber, bei, her, hei functions. The solution (5.6) holds for any value of p except $p=2$, for which case it degenerates into a single term $(z_0\pm z)^m$ with $m(m+1)=inq$.

In this investigation we shall be mostly employing the $p=\frac{4}{3}$ profile in the individual layers, which has the mathematical advantage that all the modified Bessel functions in (5.6) reduce to elementary forms; namely

$$J_{-\frac{1}{3}}[x_n(1+i)]=(2/\pi x_n)^{\frac{1}{2}}\exp\left[x_n(1-i)-\frac{\pi i}{8}\right], \quad (5.6a)$$

$$H_{-\frac{1}{3}}[x_n(1+i)]=(2/\pi x_n)^{\frac{1}{2}}\exp\left[-x_n(1-i)-\frac{\pi i}{8}\right], \quad (5.6b)$$

where $x_n=3(nq/2K_0)^{\frac{1}{2}}(z+z_0)^{\frac{1}{3}}$. For comparison we shall also analyze the linear profile with $p=1$, which is considered to be representative of the normal turbulence near the boundary while the $p=\frac{4}{3}$ profile is representative of the convective regime (Sutton, 1953; Priestley, 1959). However, it should be pointed out that our employment of these profiles is for mathematical expediency only, i.e., in finding the overall K profile that yields the best result under non-steady conditions, and is not concerned with the exact relations that must exist between the K and the θ profiles under steady conditions.

In the subsequent development of the theory with different models we shall write the nth harmonics of the temperature and the flux waves of the surface layer as

$$\theta_n=\theta_{n0}M_n(z)\cos(nqt-e_n-\alpha_n), \quad (5.7)$$

$$f_n=\theta_{n0}N_n(z)\cos(nqt-e_n+\beta_n), \quad (5.8)$$

where θ_{n0} and e_n are the amplitude and phase of the nth harmonic of the surface temperature wave and M_n, α_n, N_n, and β_n are the relative amplitudes and phases of the temperature and the heat-flux waves, respectively. By definition, we have $M_n(0)=1$ and $\alpha_n(0)=0$.

When these forms of the solutions are used, we find from (3.18b), when the absorption of solar radiation by the atmosphere is neglected by setting $B=0$, that θ_{n0} and e_n are given by

$$\tan e_n=\frac{N_{n0}\sin\beta_{n0}+N_{n0}'\sin\beta_{n0}'}{N_{n0}\cos\beta_{n0}+N_{n0}'\cos\beta_{n0}'+h}, \quad (5.9a)$$

$$\theta_{n0}=\frac{S_0b_n\cos e_n}{N_{n0}\cos\beta_{n0}+N_{n0}'\cos\beta_{n0}'+h}, \quad (5.9b)$$

where N_{n0} and β_{n0} are the surface values of N_n and β_n, while N_{n0}' and β_{n0}' are the corresponding quantities for the ground. Here the parameters $N_{n0}\cos\beta_{n0}$ and $N_{n0}'\times\cos B_{n0}'$ in (5.9a) are equivalent to the λ_n and λ_{en} in the solutions (4.2) and (4.3), but they are given in terms of the physical parameters by the solution of the problem.

We mention that, when the influence of the direct solar radiation absorbed in the atmosphere is included, the relations (5.9a, b) should be modified as in (4.6) and (4.7).

Before endeavoring to derive the solutions for the multi-layer model, let us first examine the influence of the increase of K with height by using a single-layer, $p=\frac{4}{3}$ model and compare the results with the approximate solution (5.2).

a. Model 1a. This is a single-layer, $p=\frac{4}{3}$ profile, assumed to hold for the whole half-space $z>0$. When this profile is supposed to hold for the whole half-space, the constant A in (5.6) must be set to zero in order to to keep θ_n from becoming infinite. Hence, θ_n and N_n are given by

$$\theta_n'=\theta_{n0}\left(\frac{x_{n0}}{x_n}\right)\exp[-x_n']\cos(nqt-e_n-x_n'), \quad (5.10)$$

$$N_n=\left(\frac{\bar{\rho}c_pK_0z_0^{\frac{1}{3}}}{3}\right)\exp[-x_n'](1+2x_n+4x_n^2)^{\frac{1}{2}}, \quad (5.11)$$

where $x_n=3(nq/2K_0)^{\frac{1}{2}}(z+z_0)^{\frac{1}{3}}$, $x_n'=(x-x_{n0})$, x_{n0} is the surface value of x_n, and

$$\tan\beta_n=\frac{x_n\cos x_n'-(1+x_n)\sin x_n'}{(1+x_n)\cos x_n'+\sin x_n'}. \quad (5.12)$$

We note in the solution (5.10) that the amplitude decreases with height as $x_n^{-1}\exp(-x_n')$, while the phase β_n increases as x_n'. Hence, in this model the amplitude decreases more rapidly while the phase increases less rapidly with height than the model with a constant K, just as revealed by the approximate solution (5.2). The influence of the value of dK/dz on the attenuation rate is illustrated by the curves labeled a_1, a_2 and a_3 in Fig. 3a which represent the vertical variations of the amplitude M_1 and phase α_1 of the first harmonic for the three profiles a_1, a_2 and a_3 in Fig. 3c. It is seen that the larger the value of $K^{-1}\,dK/dz$, the faster M_1 decreases and α_1 increases with height.

As for the "effective heat capacity" N_{n0}, (5.9) indicates that it is determined mainly by the factor $K_0z_0^{\frac{1}{3}}$ which measures the rate of increase of K with height at the surface, and it is rather insensitive to the surface value of K itself since x_0 is usually small. Thus, even though the surface value of K for the profile a_2 in Fig. 3c is 2000 times that for the profile a_1, the corresponding values of N_0 differ only by about one order of magnitude (see Table 3). Hence, these results confirm our previous findings from the approximate solution (5.2).

In contrast to the heat capacity parameter N_{n0}, the phase lag β_{n0} of the surface heat flux depends critically on x_{n0} and therefore on the surface value of K, as can

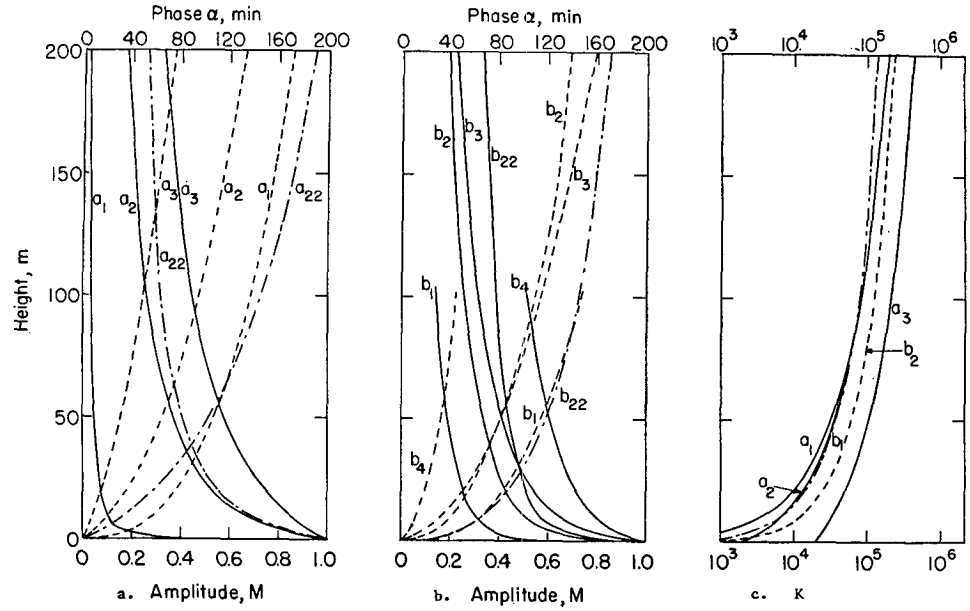

FIG. 3. Variations of relative amplitude M_1 and phase α_1 of the first harmonic for various K profiles: a., curves a_1, a_2, a_3, for single-layer, $p=\frac{4}{3}$ K-profiles with characteristics given in Table 3, curve a_{22} for a two-layer profile with the same K as a_1 below 200 m and K=constant above; b., curves b_1, b_2, b_3 for single-layer, linear profiles, curve b_{22} for a two-layer profile with the same K as b_2 below 100 m and constant above; c., the variations of K with height used in Figs. 3a and 3b.

be seen from the relation (5.12). Further, as is seen from Table 3, the values of β_{10} given by these solutions are much smaller than the value $\pi/4$ given by the constant-K model, indicating that one effect of the increase of K with height is to reduce the phase of the surface heat-flow wave.

From (5.9) we also notice that N_n decreases only very slowly with height because of the compensating effects of the two factors. This is to be expected since the heating rate is relatively low, and hence the divergence of the heat flux must be small in comparison with the flux itself.

These qualitative conclusions hold also for the solutions for other types of K profiles, such as the linear profile ($p=1$) most commonly used to represent the heat transfer by ordinary turbulence with zero buoyancy (see Haurwitz, 1936; Dorodnitsyn, 1940; Shverts, 1943; Lettau, 1951; de Vries, 1957). In these cases the solutions in (5.6) are given by the zeroth order Bessel and Hankel functions of argument $x(1+i)/2$. The variations of the amplitude M_1 and phase α_1 with height for the linear profile and different values of dK/dz are illustrated in Fig. 3b, and the corresponding values of N_{10} and β_{10} given in Table 3. It is seen that their dependence on $(dK/dz)_0$ is similar to that of the $p=\frac{4}{3}$ profiles; viz., N_{10} increases with $(dK/dz)_0$, while their dependence on $K(0)$ is relatively slight.

TABLE 3. Variations of N_{10}[10^{-4} cal cm^{-2} sec^{-1} (°C)$^{-1}$] and β_{10} [°C] with $K(0)$ and $(dK/dz)_0$ for the $p=4/3$ and $p=1$ profiles in Fig. 3.

	Curves					
	a_1	a_2	a_3	b_1	b_2	b_3
$K(0)$	1	2×10^3	2×10^4	1	12	10^3
$(dK/dz)_0$	0.636	4.00	12.33	7.2	12	7.2
N_{10}	0.476	3.72	11.60	1.68	4.12	3.68
β_{10}	2.0	12.5	12.25	7.25	10.8	15.5

b. Model 1b. In order to allow a more detailed variation of K with height and also to remove the one unrealistic feature of model 1a, i. e., K increasing indefinitely with height, we shall use a multi-layer model for more detailed calculations which are needed especially during the summer. The model is such that within each layer of finite depth, K is assumed to vary according to (5.4) with $p=\frac{4}{3}$, except in the top layer, which is assumed to be of infinite thickness and within which K is assumed to remain constant. The constants K_{0j} and z_{j0} are chosen so that K is continuous from layer to layer.

For clarity of discussion, we shall present only the detailed derivation of the solution for a two-layer K profile, with K increasing according to the $p=\frac{4}{3}$ power law from the surface to the level $z=z_1$ and remaining constant ($K=K_2=$constant) there above.

For convenience we write the solutions θ_n and f_n for the nth harmonic for the lowest layer as

$$\theta_{n1}=2\theta_{n0}\left(\frac{x_{10}}{x_1}\right)\{G_{11}\cos nt'+G_{12}\sin nt'\}, \quad (5.13)$$

$$f_{n1}=N_n(x)\cos(nt'+\beta_n), \quad (5.14)$$

$$N_n(x)=\left(\frac{2\bar{\rho}c_pK_0z_0^{\frac{1}{3}}}{3}\right)\theta_{n0}(H_{11}^2+H_{12}^2)^{\frac{1}{2}}, \quad (5.14a)$$

where

$$\tan\beta_n=-H_{12}/H_{11},\ nt'=nqt-e_n.$$

Here the various quantities have the same meanings as before, and the functions G_{11}, G_{12}, H_{11}, H_{12} are given by

$$G_{11}=A_r cS+A_i sC+\frac{\exp[-x_1']}{2}c, \tag{5.15a}$$

$$G_{12}=-A_r sC+A_i cS+\frac{\exp[-x_1']}{2}s, \tag{5.15b}$$

$$H_{11}=A_r[cS-x_1(cC-sS)]+A_i[sC-x_1(sS+cC)]+\frac{\exp[-x_1']}{2}[c+x_1(c+s)], \tag{5.15c}$$

$$H_{12}=A_r[x_1(cC+sS)-sC]+A_i[cS-x_1(cC-sS)]+\frac{\exp[-x_1']}{2}[s-x_1(c-s)], \tag{5.15d}$$

where $s=\sin x_1'$, $c=\cos x_1'$, $S=\sinh x_1'$, $C=\cosh x_1'$, and x_1 and x_1' are as defined in (5.11)

The solutions θ_{n2} and f_{n2} for the upper layer of constant $K=K_2$ are given by

$$\theta_{n2}=\theta_{n0}\exp[-z_n'][(c_r\cos z_n'-c_i\sin z_n')\cos nt'+(c_r\sin z_n'+c_i\cos z_n')\sin nt'], \tag{5.16a}$$

$$f_{n2}=\bar{\rho}c_p\left(\frac{nqK_2}{2}\right)^{\frac{1}{2}}\theta_{n0}\exp[-z_n']\times\{[(c_r+c_i)\cos z_n'+(c_r-c_i)\sin z_n']\cos nt'+[(c_r+c_i)\sin z_n'-(c_r-c_i)\cos z_n']\sin nt'\}, \tag{5.16b}$$

where $z_n'=(nq/2K_2)^{\frac{1}{2}}(z-z_2)$.

The four as yet unspecified constants A_r, A_i, c_r, and c_i are determined by the continuity requirements for θ_n and f_n at $z=z_1$, which yield:

$$2\frac{x_{10}}{x_{11}}G_{11}(z_1)=c_r, \tag{5.17a}$$

$$2\frac{x_{10}}{x_{11}}G_{12}(z_1)=c_i, \tag{5.17b}$$

$$2\frac{x_{10}}{x_{11}^2}H_{11}(z_1)=c_r+c_i, \tag{5.17c}$$

$$2\frac{x_{10}}{x_{11}^2}H_{12}(z_1)=-c_r+c_i. \tag{5.17d}$$

Substituting c_r and c_i from (5.17a, b) into (5.17c, d) we then obtain the two following equations in A_r and A_i:

$$b_1A_r+b_2A_i=2^{-1}e^{-x_{11}'}\cos x_{11}', \tag{5.18a}$$

$$-b_2A_r+b_1A_i=2^{-1}e^{-x_{11}'}\sin x_{11}', \tag{5.18b}$$

where $x_{11}=3(nq/2K_0)^{\frac{1}{2}}(z_1+z_0)^{\frac{1}{3}}$, $x_{11}'=(x_{11}-x_{10})$, and

$$\left.\begin{aligned}b_1&=x_{11}e^{x_{11}'}(\cos x_{11}'-\sin x_{11}')-\cos x_{11}'\sinh x_{11}'\\ b_2&=x_{11}e^{x_{11}'}(\cos x_{11}'+\sin x_{11}')-\sin x_{11}'\cosh x_{11}'\end{aligned}\right\}.$$

From (5.15c, d) we find that the surface values of H_1 and H_{12} are given by

$$\left.\begin{aligned}H_{11}(0)&=(\tfrac{1}{2}-A_r-A_i)x_{10}+1\\ H_{12}(0)&=(A_r-A_i-0.5)x_{10}\end{aligned}\right\}. \tag{5.19}$$

Thus, the values of N_{n0} and β_{n0} can readily be obtained from these solutions when A_r and A_i are known.

On substituting these values and the values of N_{n0}' and β_{n0}' for the lower medium in (5.9a, b) (or their modified forms when the absorption of solar radiation is included), we then obtain e_n and the ratio $L_{n0}=\theta_{n0}/(S_0b_n)$ for every n. The surface temperature can then be obtained by multiplying L_{n0} by $S_0b_n\cos(nqt-e_n)$ and summing up of all n, while the temperature changes at the upper levels are obtained by multiplying each term by the corresponding $M_n(z)$ and adding $\alpha_n(z)$ to e_n.

This model can readily be extended to any number J of layers without difficulty. When J is large, the solution is most conveniently expressed in matrix form and in terms of the quantities of the surface layer, so that L_{n0} and e_n are still given by (5.9a, b) or their equivalent forms when the direct solar radiation is taken into consideration. On calculating from this model with two and three layers we find that the influence of the vertical variation of K on the amplitude M and phase α of the temperature wave may be summarized as follows:

1) With the same K in the lowest layer, larger K at higher levels has the effects of i) giving rise to a more rapid attenuation of the amplitude M with height, ii) producing a larger amplitude N_n for the heat flux, iii) giving a smaller β_{n0}, and iv) causing either an increase or a reduction of the phase $\alpha(z)$, depending on the K profile in the lower layer.

Fig. 4b illustrates the influence of the different high-level K on the amplitude M and the phase α. For the two different pairs of K profiles c_1 and c_2, an increased K causes α to increase except below the 30-m level, where a slight reduction is produced, while for the profiles d_1 and d_2, the larger high-level K causes α to decrease below the $z=100$-m level and to increase there above. The values of N_{10} for c_1 and c_2 are 5.66×10^{-4} and 4.35×10^{-4} cal cm^{-2} sec^{-1} (°C)$^{-1}$, respectively, while the corresponding values of β_{10} are 27.4° and 49.1°, respectively. The corresponding values of N_{10} and β_{10} for d_1 and d_2 are 3.27×10^{-4} and 3.55×10^{-4} cal cm^{-2} sec^{-1} (°C)$^{-1}$ and 38.1° and 24.1°, respectively.

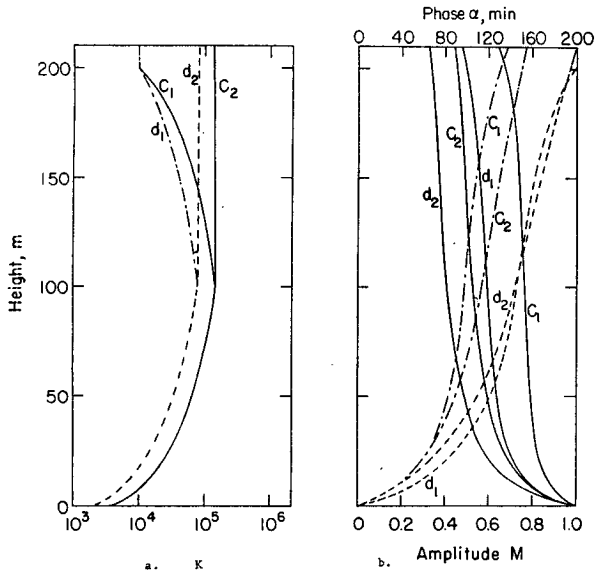

FIG. 4. The various two- and three-layer profiles used to examine the influence of the higher level K values, a., and the corresponding amplitude and phase distributions for the first harmonic, b.

2) With the same values of $K(0)$ and K_3, a higher K_{11} at the mid-level produces the effects of i) making M decrease more slowly with height above z_1, ii) giving a smaller phase lag α_1 at all levels, iii) producing a larger N_{10}, and iv) giving a smaller β_{10}.

Since all these influences are as expected from the increased K in the mid-layer, they need not be demonstrated with examples.

The information gained from the examination of the various examples are of great help in finding the profiles that fit the observed distributions of amplitude M and phase α at various stations, and a few of these examples are illustrated in Fig. 4b. The corresponding K profiles are represented in Fig. 4a.

It may be noted that the observed amplitudes and phase distributions at Leafield, England, and at Ismailia, Egypt, during December, are very well fitted by simple single-layer profiles; namely, one with $K(0)=2\times10^3$, $K_0z_0^{\frac{1}{3}}=2.98$ for Leafield and one with $K(0)=1.6\times10^3$, $K_0z_0^{\frac{1}{3}}=1.6$ for Ismailia. Those for the summer months require more complex K profiles to fit them. Thus, even though the observed values of the phase α_1 are not quite reliable, we may still conclude that during the winter the K distribution can be approximated by the single-layer $p=\frac{4}{3}$ profile up to a few hundred meters.

It may be mentioned that all the calculations show that the amplitude N_n of the heat flow wave decreases only slightly with height within the first few tens of meters from the ground. Hence, the existence of a constant heat flux layer above the surface may be assumed to be valid if one is merely using the known flux at a certain level to estimate the flux at an adjacent level.

6. The influence of the time variation of K

When the temporal variation of K is included, Eqs. (3.8) are no longer independent of one another and their exact solutions can be obtained only be treating them simultaneously. However, when the variable part K' of K is relatively small in comparison with the time-independent part $\bar{K}$, the approximate solutions of these equations can be obtained by a perturbation method, by expanding the various quantities in powers of a small parameter ϵ which measures the ratio between K' and $\bar{K}$. Thus, to illustrate the influence of K' on the propagation of the diurnal heat wave in the atmosphere, we assume that K is given by

$$K(z,t)=\bar{K}(z)+\epsilon A(z)\cos qt, \tag{6.1}$$

where $\bar{K}$ and A are considered as of the same order of magnitude, while $\epsilon\ll1$. Further, we limit ourselves to the interactions between the zero, first and second harmonics of K and θ only. Thus, we set

$$\theta_n=\theta_{n1}+\epsilon\theta_{n2}+\cdots, \tag{6.2a}$$

$$T_n=T_{n1}+\epsilon T_{n2}+\cdots. \tag{6.2b}$$

Substituting these expansions in (3.8) for the first and the second harmonics and equating to zero the coefficients of the various powers of ϵ, and omitting the solar radiation term, we find that the ϵ^0-order terms satisfy the homogeneous equations while the ϵ-order terms of θ satisfy the following non-homogeneous equations:

$$\frac{d}{dz}\left(\bar{K}\frac{d\theta_{12}}{dz}\right)+iq\theta_{12}=-\frac{d}{dz}\left(A\frac{d\theta_0}{dz}+\frac{A}{2}\frac{d\theta_{21}}{dz}\right), \tag{6.3}$$

$$\frac{d}{dz}\left(\bar{K}\frac{d\theta_{22}}{dz}\right)+2qi\theta_{22}=-\frac{1}{2}\frac{d}{dz}\left(A\frac{d\theta_{11}}{dz}\right). \tag{6.4}$$

Similarly, on substituting the expansions (6.2a, b) in (3.18b) we find that the ϵ^0-order terms satisfy the same condition as when A is absent, while the ϵ-order terms satisfy the following relations at $z=0$:

$$-\bar{\rho}c_p\left[\bar{K}\frac{d\theta_{12}}{dz}+A\frac{d\theta_0}{dz}+\frac{A}{2}\frac{d\theta_{21}}{dz}\right]+\rho_e c K_e\left(\frac{dT_{12}}{dz}\right)+hT_{12}=0, \tag{6.5}$$

$$-\bar{\rho}c_p\left[\bar{K}\frac{d\theta_{22}}{dz}+\frac{A}{2}\frac{d\theta_{11}}{dz}\right]+\rho_e c K_e\left(\frac{dT_{22}}{dz}\right)+hT_{22}=0. \tag{6.6}$$

On the other hand, T_{12} and T_{22} satisfy the same homogeneous equations (3.12) as T_{11} and T_{21}, and hence may be taken as constant multiples of the latter.

For the first nonhomogeneous term on the right-hand side of (6.3) we observe that the mean stability $d\theta_0/dz$

given by the O'Neill observations in the first few meters near the ground is nearly zero, and it increases to about 6×10^{-5}C cm^{-1} there above. Since the convective transfer vanishes above a certain height, we may adopt the following vertical distribution of $Ad\theta_0/dz$ for our three-layer $\bar{K}=K_0(z+z_0)^{\frac{4}{3}}$ model:

$$\left.\begin{aligned} &A\frac{d\theta_0}{dz}=0, \quad \text{for } 0\leqslant z\leqslant z_1\\ &A\frac{d\theta_0}{dz}=b_0'(z+z_0)-b_2'(z+z_0)^{5/3}, \quad \text{for } z_1\leqslant z\leqslant z_2\\ &A\frac{d\theta_0}{dz}=\beta z e^{-\gamma(z-z_2)}, \quad \text{for } z>z_2 \end{aligned}\right\} \tag{6.7}$$

where b'_0, b'_2, β and γ are given constants which may be determined from our estimates of A and $d\theta_0/dz$. Further, we shall take $A(z)=\bar{K}(z)$.

For this case the first particular solution of (6.3) in the three layers is given by

$$\theta_{121}^{(\mathrm{I})}=0, \tag{6.8a}$$

$$\theta_{121}^{(\mathrm{II})}=\frac{10K_0}{9q^2}(b_2'\cos qt)+\left(\frac{b_0'}{q}-\frac{5b_2'}{3q}(z+z_0)^{\frac{4}{3}}\right)\sin qt, \tag{6.8b}$$

$$\theta_{121}^{(\mathrm{III})}=\exp[-\gamma(z-z_2)](a_{0r}+a_{1r}z)\cos qt+(a_{0i}+a_{1i}z)\sin qt, \tag{6.8c}$$

where

$$\mu=q/K_3,$$

$$a_{0r}+ia_{0i}=\frac{\beta}{K_3(\gamma^4+\mu^2)^2}[\gamma^6-3\mu^2\gamma^2-i(3\gamma^4-\mu^2)],$$

$$a_{1r}+ia_{1i}=\frac{\beta^2}{K_3(\gamma^4+\mu^2)}(\gamma^2-i\mu).$$

For the case $A=\bar{K}$ it is readily found that the particular solution corresponding to the second term on the right-hand side of (6.3) is given by

$$\theta_{122}=-\tfrac{2}{3}\theta_{21}. \tag{6.9}$$

Thus, the complete solution of (6.3) may be written as

$$\left.\begin{aligned} \theta_{12}'&=\epsilon(C_1\theta_{11}-\tfrac{2}{3}\theta_{21}+\theta_{121})\exp[-i(qt-e_1')]\\ T_{12}'&=\epsilon C_2T_{11}\exp[-i(qt-e_1')] \end{aligned}\right\}, \tag{6.10}$$

where θ_{11}, θ_{21} and T_{11} are solutions of the homogeneous equations and C_1, C_2 and e_1 are determined by the conditions (3.18a) and (6.5). Thus, for constant $\bar{K}=A$ we find

$$\left.\begin{aligned} C_2&=-\frac{0.2929\lambda_1}{(\lambda_1+\lambda_{e1})}\frac{\theta_{20}}{\theta_{10}}\\ C_1&=\left[1-\frac{0.2929\lambda_1}{(\lambda_1+\lambda_{e1})}\right]\frac{\theta_{20}}{\theta_{10}}\\ e_1'&=\pi/4 \end{aligned}\right\}. \tag{6.10a}$$

The solution θ_{22} can be obtained in a similar manner, which we shall not discuss in this paper as it is not very significant for the diurnal heat wave.

It may be mentioned that the ratio θ_{20}/θ_{10} is always small, hence the first two terms on the right side of (6.10) may be taken as of second order in ϵ and neglected when ϵ is small, so that θ_{12} is given by θ_{121} alone.

7. The variation of the mean temperature with height

Under steady conditions the variation of the mean temperature with height is governed by (3.7), which, for the layer with $\bar{K}_0=K_0(z+z_0)^{\frac{4}{3}}$, may be written as

$$\frac{d^2\theta^*}{dx^2}+\frac{2}{x}\frac{d\theta^*}{dx}-\theta^*=-\frac{1}{\rho c_p a^2}\frac{d}{dz}(\cos uS)_0-\frac{1}{8a^2}\sum_{n=1}^{\infty}\frac{d}{dz}\left(A_n\frac{d\theta_n^{(c)}}{dz}\right), \tag{7.1}$$

where $x=3a(1/K_0)^{\frac{1}{3}}(z+z_0)^{\frac{1}{3}}$ and $\theta^*=\theta_0-\bar{\theta}$. As has been discussed in Section 3, the first term on the right-hand side of this equation varies only slightly with height within the first few hundred meters of the atmosphere, and hence the particular solution corresponding to this term may be taken as $\theta_{0s}=T_{es}(P/p)^{R/c_p}$, which represents the equilibrium constant temperature when the absorption of solar radiation is balanced by the Newtonian cooling.

The particular solution θ_{2p}^* corresponding to the interaction terms can be obtained either analytically or numerically when A_n and $\theta_n^{(c)}$ are known. Hence, the total solution of (7.1) may be written as

$$\theta_0=\bar{\theta}+\theta_{0s}+\theta_{2p}^*+(1/x)(C_1e^{-x}+C_2e^{x}), \tag{7.2}$$

where C_1 and C_2 are unspecified constants, to be determined by the continuity requirements and the boundary conditions (3.18a, b) specialized to the mean temperatures T_{e0} and θ_0.

For simplicity, let us restrict ourselves to the case where the $p=\frac{4}{3}$ profile extends to $z=\infty$. Then the constant C_2 must be set to zero. Further, we shall assume that there is no mean heat flow at great depths in the ground and $K_e=$ constant. Then the mean temperature T_{e0} of the ground must be a constant and the conditions

(3.18a, b) yield the following two relations at $z=0$:

$$T_{e0}=\bar{\theta}+\theta_{0s}+\theta_{2p}{}^{*}+C_1\frac{e^{-x_0}}{x_0}, \tag{7.3}$$

$$\rho c_p a K_0{}^{\frac{1}{2}} z_0{}^{\frac{1}{2}}\frac{d}{dx}\left[C_1\frac{e^{-x}}{x}+\theta_{2p}{}^{*}\right]+\bar{F}=0, \tag{7.4}$$

where $\bar{F}$ stands for the total downward flux of energy at the surface. Thus, (7.4) determines C_1 in terms of the radiation and other physical parameters while (7.3) determines the mean surface temperature difference $T_{e0}-\bar{\theta}$.

To illustrate the nature of this solution, let us take into consideration only the first harmonic in $\theta_{2p}{}^{*}$, i.e., $\theta_{2p}{}^{*}=-\theta_1/8$, and assume $S_0 b_1=2\bar{F}$, $q\gg a^2$. We then find that the solution (7.2) is approximately given by

$$\theta^{*}=T_{as}(P/p)^{R/c_p}p+\left(\frac{9\bar{F}a}{4\rho c_p}\right)\left(\frac{1}{K_0{}^3}\right)^{\frac{1}{4}} \times\frac{1}{x}\left(3e^{-x}-\exp\left[-\frac{\sqrt{q}x}{a}\right]\right). \tag{7.2a}$$

When a multiple-layer model is used to represent the variation of $\bar{K}$ with height, the C_2e^{x}/x term must be included in the solution (7.2) for the lower layers, while for the top layer of constant K both the particular solution $\theta_{2p}{}^{*}$ and the complimentary solution are given by decreasing exponential functions, viz.,

$$\left.\begin{aligned}\theta_{2p}{}^{*}&=-\frac{1}{8K}\sum_{n=1}^{\infty}A_n\theta_n\left(\frac{nq}{nq-a^2}\right)\\ \theta_c{}^{*}&=C_1\exp[-azK^{-\frac{1}{2}}]\end{aligned}\right\}. \tag{7.5}$$

The solutions (7.2a) and (7.5) show that the mean potential temperature profile given by the present model is controlled by three processes: short- and longwave radiation, and convective-turbulence transfer. The first process creates a stable, nearly isothermal stratification, while the two latter processes produce a boundary-layer type, unstable stratification. Thus, when the surface insolation is strong, the net effect of these processes is to maintain a stable mean lapse rate above a thin boundary layer, within which the mean lapse rate may be nearly adiabatic or unstable.

The analysis can be generalized to non-steady conditions by equating the difference between the two sides of (7.1) to the rate of change of θ_0 instead of to zero. Then $\theta_0(z,t)$ is given by a partial differential equation which is equivalent ot (3.4), but with nonhomogeneous terms representing the net heat transfer produced by the diurnal variations present.

It should be mentioned again that for comparison with individual observations the influence of advection by mean motion must be taken into consideration, especially for the mean temperature distribution.

8. Comparison between theoretical calculations and the O'Neill and other observations

a. Diurnal temperature waves in summer

To examine how well our modified virtual conduction model can predict the diurnal temperature wave in the atmosphere and in the ground, let us first try to find a solution that fits the O'Neill observation in Fig. 1c and another solution for the average observation in Fig. 1b. For these cases we take $H=13\pi/24$, which corresponds to a 13-hr day, and assume a two-layer ground with K_e increasing from $K_e(0)$ at the surface to $K_e(z_1)$ at the depth z_1, and remaining constant farther downward. This variation of K_e approximates closely the measured variations of K_e during the third period of observation and is also close to the average conditions. Since calculations show that the results given by this variable K_e model are in every respect better than that given by the constant K_e model, we shall use it in all the subsequent developments. Further, we shall assign the surface radiation factor h the constant value 1.08×10^{-4} cal cm^{-2} sec^{-1} (°C)$^{-1}$, which appears to be representative of the summer situation.

As has been discussed in the preceding sections, the diurnal temperature waves in the atmosphere are directly influenced by the absorption of solar radiation in the atmosphere and by the convective heat transfer, which are represented by the first and the second terms on the right-hand side of (3.8), respectively. Through the relations (4.4a–d) these influences are also felt in the ground. In order to investigate the influences of these nonhomogeneous terms quantitatively, we shall omit them first and then introduce them afterward one by one. Thus, as our first example we have in Fig. 5 the solutions of the homogeneous part of (3.8) for the three-layer K profile with $K_{10}=400$, $K_{11}=10^5$, $K_3=5\times10^5$ cm^2 sec^{-1}, $z_1=10$ m, $z_2=200$ m, where the amplitude at the -0.5-cm level has been set to the observed value in Fig. 1b. On comparing these temperature curves with those in Figs. 1b and 1c, we notice the similarity between the theoretical and the observed variations. Further, the calculated variations at the -0.5-cm level agree with the observed variations very closely. However, the calculated amplitudes at the other levels are too large and the phase changes are too slow above the ground in comparison with the observed variations in Figs. 1b and 1c, and therefore these solutions are not showing sufficiently the boundary-layer nature of the temperature variation. These discrepancies between the theory and observations cannot be removed by modifying the vertical variations of K alone, especially the phase deviations, even though the low level amplitude can be reduced by taking a smaller K_{10}.

A significant improvement of the results for the lowest 10–20 m is obtained by including the first nonhomogeneous term on the right-hand side of (3.8), which arises from the absorption of solar radiation, and by reducing

the surface value of K. The influences of the solar radiation term are to 1) increase the amplitude of the temperature wave at higher levels, 2) shift the temperature maxima backward, and 3) increase the cooling rate during the night. This last influence is compensated by the reduction of the value of K_{10}, so that the correct surface temperature change can be achieved by taking a smaller K_{10}. Thus, for the 24–25 August observations we find that the best results are obtained by the three-layer atmospheric model with $K_{10}=3$, $K=10^5$, $K_3=5\times10^5$ cm^2 sec^{-1}, $z_1=10$ m, $z_2=200$ m, and $B_n'=200/n$ (°C) cm^2 sec cal^{-1}, which corresponds to an about 10% absorption of the solar radiation in the atmosphere. The temperature variations given by this solution at the lower levels, from -0.005 to 16 m are represented in Fig. 6, with the observed mean lapse rate superimposed, while those at the 100-, 200- and 400-m levels are represented by the curves marked b in Fig. 7, It is seen that these results agree quite well with the observations in Fig. 1c up to the 16-m level, while above the 100-m level the calculated variations lag behind the observed distributions. Here again we find that the discrepancies cannot be removed by merely changing the vertical distribution of K at these and still higher levels, and the next factor to take into consideration is the first-order interaction term on the right-hand side of (3.8) arising from the convective activity. By taking $b_0'=1.1\times10^5$ C sec^{-1} and $b_1'=6qb_0/K_{02}$ in the expression $Ad\theta_0/dz$ of (6.7) for the second layer (10 m$\leq z\leq$200 m), we then find that $\theta_{12}^{(II)}$ is given by

$$\theta_{12}^{(II)}=\cos qt+0.15\left[1-1.667\left(\frac{z+z_0}{\bar{z}+z_0}\right)^{\frac{1}{3}}\right]\sin qt, \quad (8.1)$$

where $z_0=71.07$ m and $K_{02}=0.614$ are the two parameters of the K profile in the second layer, and $\bar{z}$ is the

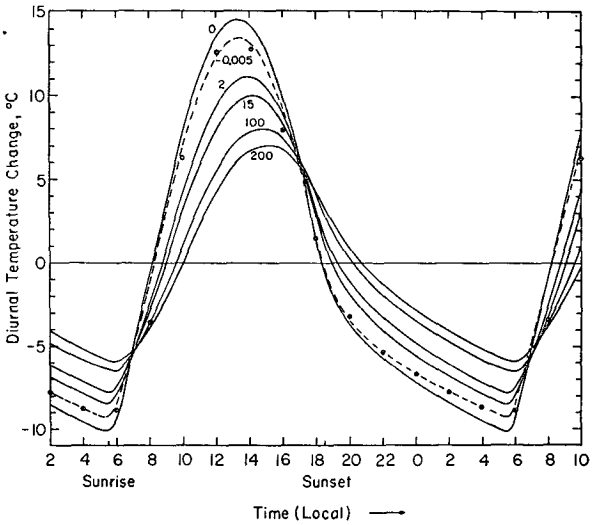

FIG. 5. Theoretical predictions of the diurnal temperature variations at various levels from the three-layer, pure conductive model for $K_{10}=400$, $K_{11}=10^5$, $K_3=5\times10^5$ cm^2 sec^{-1}, $z_1=10$ m, $z_2=200$ m.

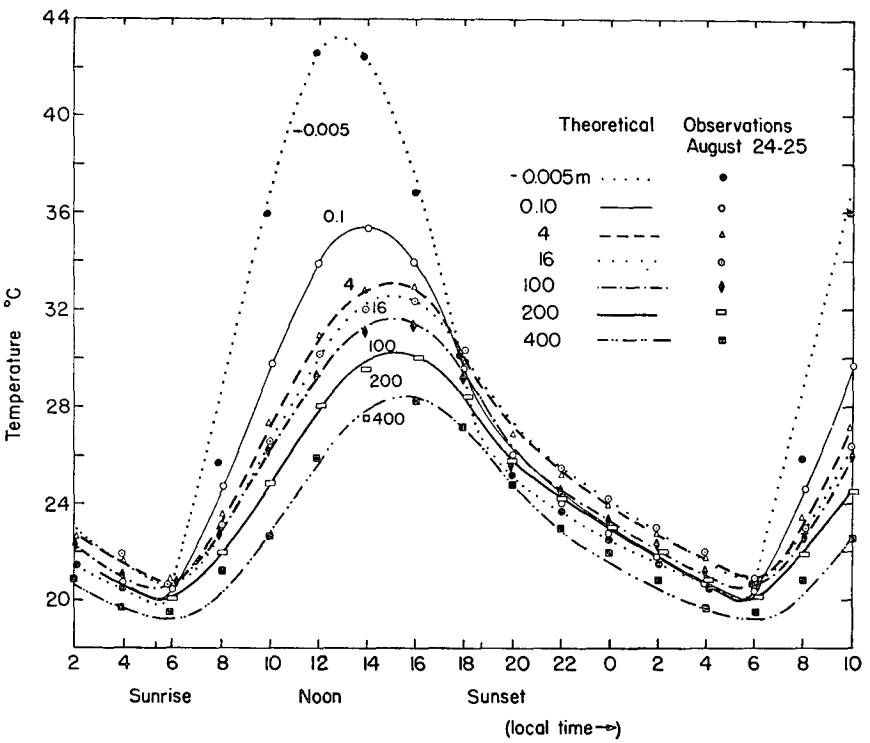

FIG. 6. Theoretical predictions of diurnal temperature variations from radiative-convective model and comparison with observations at O'Neill, Nebr., 24–25 August 1953.

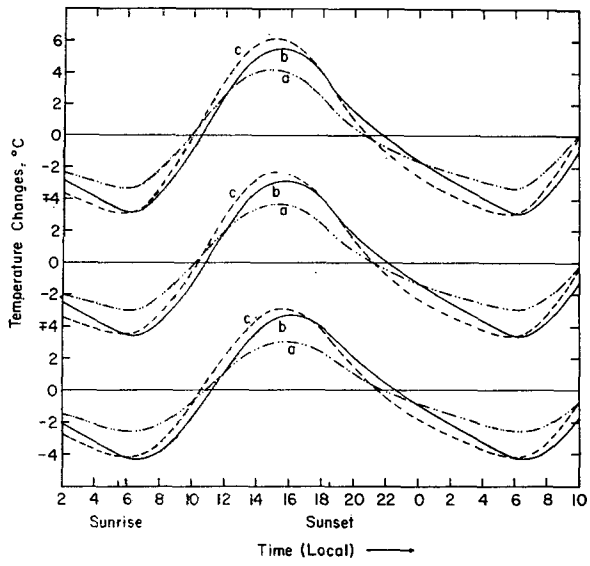

FIG. 7. Contributions from absorption of solar radiation (curves b) and K-T interaction (curves c) at the 100- 200- and 400-m levels.

height at which $Ad\theta_0/dz$ becomes negligible, which we have taken as 500 m.

The variation of this function at the 100-, 200- and 400-m levels, when added to the corresponding solutions b in Fig. 7, are represented in Fig. 6. From these results we see that the calculated temperature waves at the above mentioned levels are also brought into good agreement with the observations. It may be mentioned that the value of A used at the 100-m level for the present case is only about 5000 cm^2 sec^{-1}, which is much smaller than the corresponding value $\bar{K}$. Hence, the perturbation method is valid.

Similarly, we find that the average observations in Fig. 1b can be represented fairly closely by the solution of (3.8) for a three-layer K profile with $K_{10}=5$, $K_{11}=10^5$, $K_3=5\times10^5$ cm^2 sec^{-1}, $z_1=10$ m and $z_2=200$ m. Here again it is necessary to take into consideration the solar radiation term $[B_n'=150/n$ (°C) cm^2 sec cal$^{-1}]$ and the K-T interaction term, but with a somewhat smaller amplitude and not extending above the 200-m level, reflecting the fact that convection is less fully developed on the average than during the fifth and sixth periods of observations. The results so obtained are represented in Fig. 8. As is to be expected, the agreement between the calculated and the observed values for this case is not as close as in the previous example, since the average observations are interrupted by many other disturbances.

The diurnal temperature variations in the ground as given by the two-layer model with K_e increasing from the surface value $K_e(0)=1.51\times10^{-3}$ cm^{-2} sec^{-1} to $K_e=7.18\times10^{-3}$ cm^2 sec^{-1} at $z=10$ cm according to the $K_e=K_0\,(z+z_0)^{\frac{1}{2}}$ formula, and remaining constant farther below, with the solar radiation factor $B'=150/n$ (°C) cm^2 sec cal^{-1}, are superimposed on the mean lapse

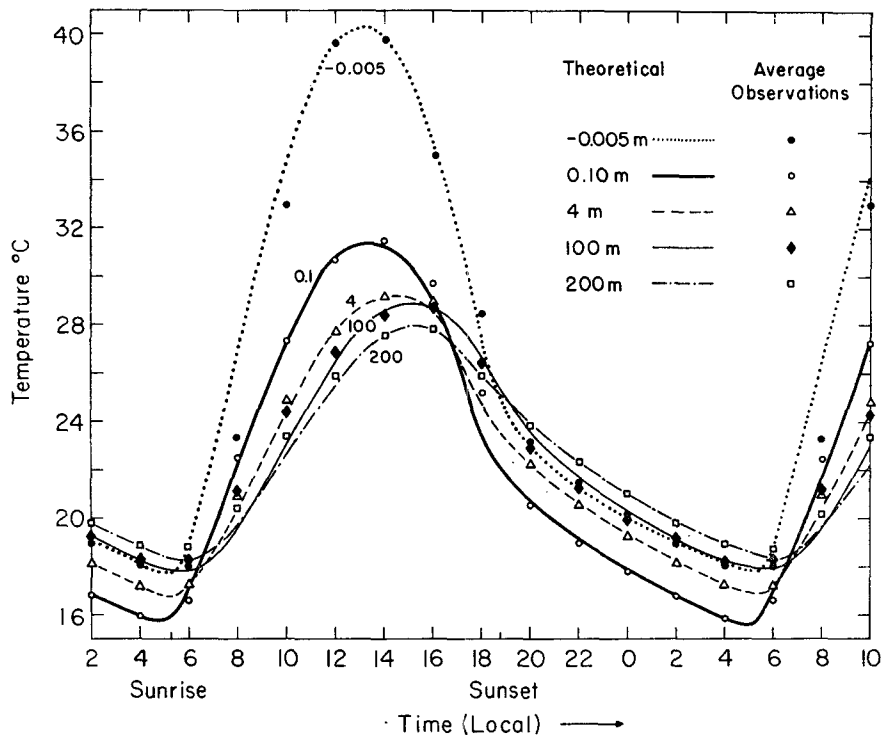

FIG. 8. Comparison between theoretical predictions from the complete radiative-conductive model of the average diurnal temperature variations at O'Neill, Nebr., and observations.

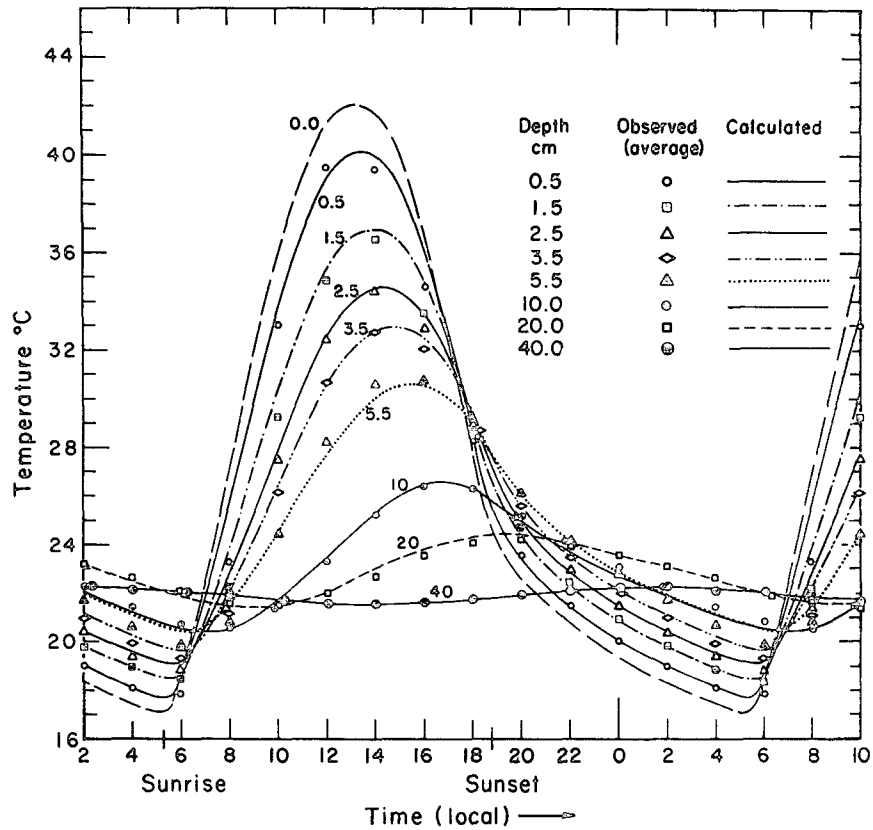

FIG. 9. Variations of soil temperature based on calculations from the two-layer model. Data are mean observations.

rate and plotted in Fig. 9, together with the mean observations represented in Fig. 1a. It is seen that the theoretical results and the observations agree quite well, both in amplitude and in phase, especially during the night. Hence, we may conclude that the changes of the soil temperature during the night can be predicted quite accurately by the present model, although the same accuracy can not be achieved for the early morning without more adequate knowledge about the soil properties and the evaporation process.

In the above comparisons the amplitude of the temperature wave at $z=-0.5$ cm has been fitted to the observed value. To determine this amplitude independently, the observed solar intensity at the surface should have been used instead. However, since S_0 and the Bowen ratio $1/m$ have not been measured accurately, only a rough comparison in this respect can be made at the present. Thus, on making use of the observed maximum hourly average downward flux of solar energy at the surface and the Bowen ratio at O'Neill during the fifth observation, which are about 1.3 cal cm^{-2} min^{-1} and 5.0, respectively, and the calculated range $\Delta\theta(0)/S_0=1390$C cm^2 sec cal^{-1}, we find

$$\Delta\theta(0)=1390\times\left(\frac{1.3}{60\times1.2}\right)=25.1\text{C}.$$

This value is to be compared with the observed average value $\Delta\theta(0)=25.4$C obtained from the observed amplitude 23.1C at $z=-0.5$ cm. Thus, the calculated average temperature range is very close to the observed range, and therefore, the theoretical results may also be considered as correct in the absolute sense.

It should be mentioned that the calculated values of T at $z=-0.5$ cm during the morning are always higher than the observed values, even though good agreement between theory and observations are obtained for other parts of the day and at other levels. Judging from the fact that quite large differences are recorded by the different instruments during the morning when the temperature is rising rapidly, we suspect that a major part of this discrepancy may be attributable to the slow response of the instrument to the rising temperature. On the other hand, part of the discrepancy may also be attributed to evaporation from the topmost layer of the earth, and another part attributed to the difference between the actual solar intensity at the surface and that given by the relations (3.11), (3.12) and (3.17), as is manifested by the observed surface insolation at Toronto given by Munn (1966). Thus, by using the observed values of S_0 at Toronto but reducing them to a 13-hr day, the difference between the calculated and the observed T at 1000 is reduced from 2 to 1C.

Similarly, the variations of the amplitude and phase with height observed at Seattle, Wash., during August as given Staley (1956), can be represented fairly closely by the solution of (3.8) for a three-layered K profile, as can be seen from the curves labeled as S in Fig. 10a. However, here the observed very slow increase of phase above 10 m indicates that the solar radiation and convective interaction terms are also of importance. Since no detailed observations are available, the corresponding higher harmonics have not been calculated.

b. The diurnal temperature waves in winter

During the winter the surface heating rate is low and the day is short; hence, no intense thermal boundary layer will form and strong thermal convection due to surface heating is absent. Under these circumstances part of the absorption spectrum of the atmosphere falls into the strongly absorbed category discussed in Section 3, and hence it gives rise to a relatively large radiative diffusivity, making the surface value of the virtual conduction coefficient K much larger than that due to turbulence alone. Consequently, the temperature wave changes much more slowly with height in winter and the vertical variations of the amplitude and phase can be represented by the solution of (3.8) for a relatively simple K profile. Further, the influences of the nonhomogeneous terms of (3.8) are relatively insignificant and may be neglected. For example, the curves labeled as L_w and I_w in Figs. 10a and 10b represent the vertical distributions of the amplitude M_1 and the phase α_1 of the first harmonic for a single-layer, $p=\frac{4}{3}$ model, with $K(0)=2\times10^3$ cm^2 sec^{-1}, $K_0 z_0^{\frac{1}{3}}=2.98$ for L_w and $K(0)=1.6\times10^3$ cm^2 sec^{-1}, $K_0 z_0^{\frac{1}{3}}=1.6$ for I_w, as represented in Fig. 10c, while the data points are the observed values of the amplitudes and phases at Leafield, England, and at Ismailia, Egypt, during December (from Sutton, 1953). It is seen that the theoretical results fit the observations very closely.

In contrast to the situations in winter, the amplitude and phase variations at these two stations in summer can only be approximated by the solutions for more complex K profiles, such as those given by the two-layer or three-layer models as illustrated by the curves labeled as L_s and I_s in Figs. 10a and 10b with the corresponding K profile given in Fig. 10c. Here K increases very rapidly to very high values within a few tens of meters from the ground, and decreases above the 200-m level with height. For Ismailia it is found that close agreement between theory and observations both in amplitude and in phase cannot be achieved by simply varying the K distribution, indicating the importance of the convective interaction term and probably also the solar radiation term. Since no detailed observations are available, detailed calculations for the higher harmonics have not been made for these stations.

9. Concluding remarks

Calculations with the radiative and conductive atmospheric temperature-change model presented above indicate that the diurnal temperature variations within the first few hundred meters of the atmosphere and in the ground during the summer, such as those observed at O'Neill by the Great Plains turbulence project, can be predicted quite accurately by using a turbulent dif-

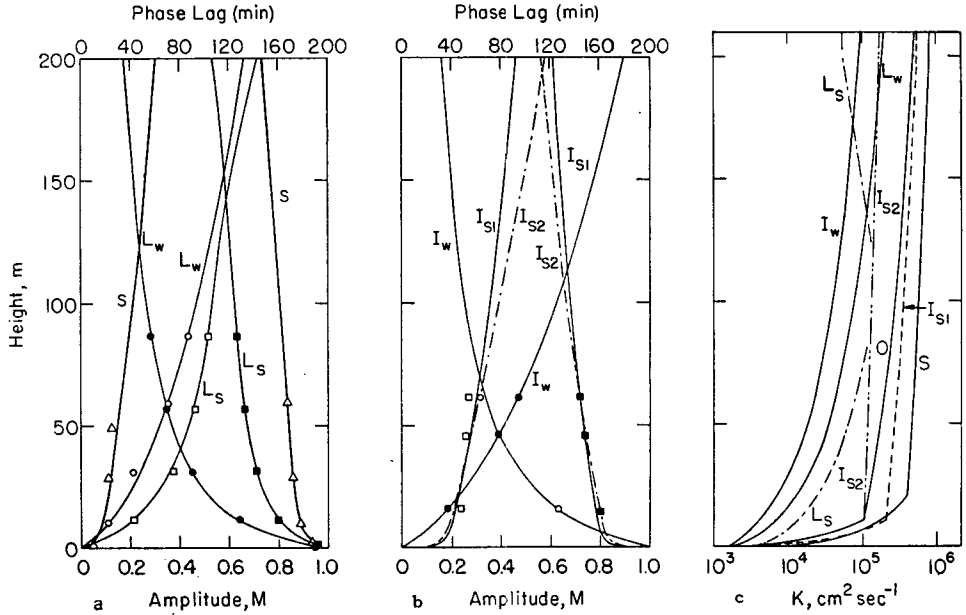

FIG. 10a, b. Calculated vertical distributions of amplitude M_1 and phase α_1 of the first harmonic from the pure conductive equation for K profiles represented in c. Data in a. are for Leafield and Seattle, those in b. are for Ismailia; s represents summer, w winter.

fusivity which increases very rapidly with height near the ground, from a very small surface value (<10 cm^2 sec^{-1}) to over 10^5 cm^2 sec^{-1} above the 10-m level, and by taking into consideration the influences of direct solar radiation and the interaction term resulting from the correlation between K and T; the winter observations can be approximated closely by the solution for a relatively simple K profile without the necessity of including the direct solar radiation and the K-T interaction terms, provided a larger surface K value of the order of 10^3 cm^2 sec^{-1} is used. Further, it is also shown that, if one is interested only in the temperature changes at the -0.5-cm level, fairly good results can be achieved by using a one-medium constant K_e model, with the K_e value properly chosen to suit the circumstance. This is especially so for the temperature changes during the night, as has been demonstrated by the works of Brunt (1932), Phillipps (1940, 1962) and Groen (1947). However, if the temperature variations at the other levels are also desired, accurate results can only be obtained from the complex model which takes into consideration the various influences properly.

On analyzing the results obtained from the present model, we find that during the summer when an intense thermal boundary layer is present and where the ground is composed of normal soil with a K_e of the order of 10^{-3} cm^2 sec^{-1}, such as that at O'Neill, most (80%) of the solar energy received by the surface is transmitted to the atmosphere, whereas during the winter under similar conditions the amount transmitted into the earth is of the same order of magnitude as that transmitted into the atmosphere. However, as the energy fluxes at the surface are in direct proportion to the respective effective heat capacities of the media, they are dependent on the thermal properties of the underlying ground, especially those of the topmost layer, as has been pointed out by Zdunkowski *et al.* (1967), as well as on the K profile in the atmosphere. Thus, over an agitated ocean surface where the effective heat capacity λ_{e1} [Eq. (4.3b)] may be as high as 60, according to Lettau (1951), the amplitude of the surface temperature change will be much smaller and most of the solar energy will be transported downward and stored up in the water.

The calculations also show that the conductive heat flux varies appreciably from level to level, in contrast to the commonly employed assumption of it being constant with height. For example, the amplitudes of the heat flux wave for the cases represented in Figs. 6 and 8 at the 400-m level are about 66% of their values at the surface, and the rate of attenuation is slightly larger near the surface than at higher levels. Thus, in this respect the present model differs very much from the numerical model employed by Estoque (1963), where a constant flux layer of 50 m thickness was assumed. It is evident that such a model will not be able to represent the temperature variations in the thermal boundary layer.

It may be pointed out that in the present investigation no attempt is made to relate the vertical distribution of K with the local values of the Richardson number or the local stability $\partial\theta/\partial z$. From the observations and the theoretical analysis presented above one gets the impression that the value of K at the level z depends not only on the local value of $\partial\theta/\partial z$, but also on the integrated stability, from the surface level up to the equilibrium level; that is, to the level where θ equals the surface value θ_s. The reason for this is that most of the turbulent elements originate either from the heated surface, or from the very unstable boundary layer, and they penetrate into the stable layers above. Thus, the rate of the convective transfer of heat at various levels must depend upon the potential temperature differences $\Delta_1\theta=\theta_s-\theta$, $\Delta_2\theta=\theta_s-\theta_m$, and $\Delta_3\theta=\theta-\theta_e$, where θ_s is the effective mean value of the surface source layer, θ_m the value of θ at the level of minimum θ, and $\theta_e=\theta_s$ the potential temperature at the level of equilibrium of the surface air. Evidently, the rate of heat transfer also depends upon the rate at which heat is being supplied at the surface. It is the author's opinion that a concerted combined statistical and dynamical approach to the study of thermal turbulence from this viewpoint is a worthwhile undertaking.

Finally, we would remark that a study of the stability of the temperature profile given by the solutions discussed above seems to be more relevant to the problem of the development of organized thermal convections in the atmosphere from solar heating at the ground, which are most probably closely related to the formations of the regular patterned shallow cumulus clouds.

Acknowledgments. This work was sponsored by the National Science Foundation under Grant No. NDF-GP-905.

Lists of Symbols

θ	potential temperature of atmosphere
T_s	temperature of ground
θ_0	daily average potential temperature
θ_n, T_n	amplitudes of the nth harmonic of θ and T_s
θ_{n0}, T_{n0}	surface values of θ_n and T_n
e_n	phase of the surface temperature wave
α_n	relative phase of the atmospheric temperature wave
K_t	turbulent thermal conductivity of atmosphere
K_r	radiative conductivity
$K=K_t+K_r$	virtual conductivity
A_m	amplitude of the mth harmonic of K
a^2, h	coefficients of Newtonian cooling of atmosphere and of ground surface
T_{as}	temperature change produced by solar radiation
B, B_n'	coefficient of solar heating
S, S_0	intensity of solar radiation and its surface value

b_n, b_n' expansion coefficients of surface solar intensity

ρC_p, $\rho_e C$ heat capacities of atmosphere and ground

λ_n, λ_{en} effective heat capacities of the atmosphere and ground for the nth harmonic of the heat wave

f_0, f_0' surface conductive heat fluxes from atmosphere and from ground

z_{j0}, K_{j0} constants of the K profile in the jth layer

N_n, β_n, N_n', β_n' amplitudes and relative phases of the nth harmonic of the heat flux waves in the atmosphere and in the ground

REFERENCES

Best, A. C., 1935: Transfer of heat and momentum in the lowest layers of atmosphere. *Geophys. Mem.*, No. 65, 66 pp.

Brunt, D., 1932: Notes on radiation in the atmosphere. *Quart. J. Roy. Meteor. Soc.*, **58**, 389–418.

——, 1939: *Physical and Dynamic Meteorology*. Second ed., Cambridge University Press, 428 pp.

de Vries, F. A., 1957: On the integration of the heat conduction equation with periodic variation of temperature. *J. Meteor.*, **14**, 71–76.

Dorodnitsyn, A. A., 1940: On the K-theory of diurnal temperature course in the mixing layer. *Dokl. Akad. Nauk. SSSR*, **30**, No. 5.

Estoque, M. A., 1963: A numerical model of the atmospheric boundary layer. *J. Geophys. Res.*, **68**, 1103–1113.

Goody, R. M., 1960: The influence of radiative transfer on the propagation of a temperature wave in a stratified diffusing atmosphere. *J. Fluid Mech.*, **9**, 445–454.

——, 1964: *Atmospheric Radiation*. London, Oxford University Press, 436 pp.

Groen, P., 1947: Note on the theory of nocturnal radiational cooling of the earth's surface. *J. Meteor.*, **4**, 63–66.

Haurwitz, B., 1936: The daily temperature period for a linear variation of the Austausch coefficient. *Trans. Roy. Soc. Canada, Section 3*, **30**, 1–8.

Jaeger, J. C., and C. H. Johnson, 1953: Note on diurnal temperature variation. *Geofis. Pura Appl.*, **24**, 104–106.

Kibel, I. A., 1943: On temperature distribution in the earth's atmosphere. *Dokl. Akad. Nauk, SSSR*, **39**, 18–22.

Kuo, H. L., 1968: A note on the radiative-conductive heat transfer equations. Tech. Rept. 14, Thermal Circulation Project, Dept. of Geophysical Sciences, Univ. of Chicago, 15 pp.

Lettau, Heinz H., 1951: Theory of surface-temperature and heat-surface oscillations near a level ground surface. *Trans. Amer. Geophys. Union*, **32**,189–200.

——, and Ben Davidson, 1957: *Exploring the Atmosphere's First Mile*. Vol. 2, New York, Permagon Press, 377–577.

McDonald, James E., 1960: Direct absorption of solar radiation by atmospheric water vapor. *J. Meteor.*, **17**, 319–328.

Mügge, R., and F. Moller, 1932: Zur Berechnung von Strahlungstromen und Temperaturanderungen in Atmosphären von beliebigem Aufbau. *Z. Geophys.*, **8**, 53–64.

Munn, R. E., 1966: *Descriptive Meteorology*. New York, Academic Press, 245 pp.

Phillipps, H., 1940: Die nachtliche Abkuhlung des Erdbodens durch Strahlung und Warmeleitung und der Bodenschicht durch Turbulenz. *Beitr. Geophys.*, **56**, 296–319.

——, 1962: Zur Theorie des Tagesganges der Temperatur in der bodennahen Atmosphare und in ihrer Unterlage. Part I. *Z. Meteor.*, **16**, 131–177; Part II, 1964: *Z. Meteor.*, **17**, 3–32.

Priestley, C. H. B., 1959: *Turbulent Transfer in the Lower Atmosphere*. University of Chicago Press, 130 pp.

Shverts, M. E., 1943: The turbulent boundary layer in the atmosphere. *Bull. Acad. Sci., USSR, Geograph. Geophys. Ser.*, No. 4, 218–244.

Staley, D. O., 1956: The diurnal temperature wave for bounded eddy conductivity. *J. Meteor.*, **13**, 13–20.

Sutton, O. G., 1953: *Micrometeorology*. New York, McGraw-Hill, 333 pp.

Zdunkowski, W. G., D. Henderson and J. V. Hales, 1967: Prediction of nocturnal temperature changes during a calm night. *Beitr. Phys. Atmos.*, **40**, 144–157.